ERL2015 Workshop, BNL-STONY BROOK UNIVERSITY, 7-12 June 2015

Beam and spin dynamics studies in eRHIC ERL

François Méot, BNL C-AD

Contents

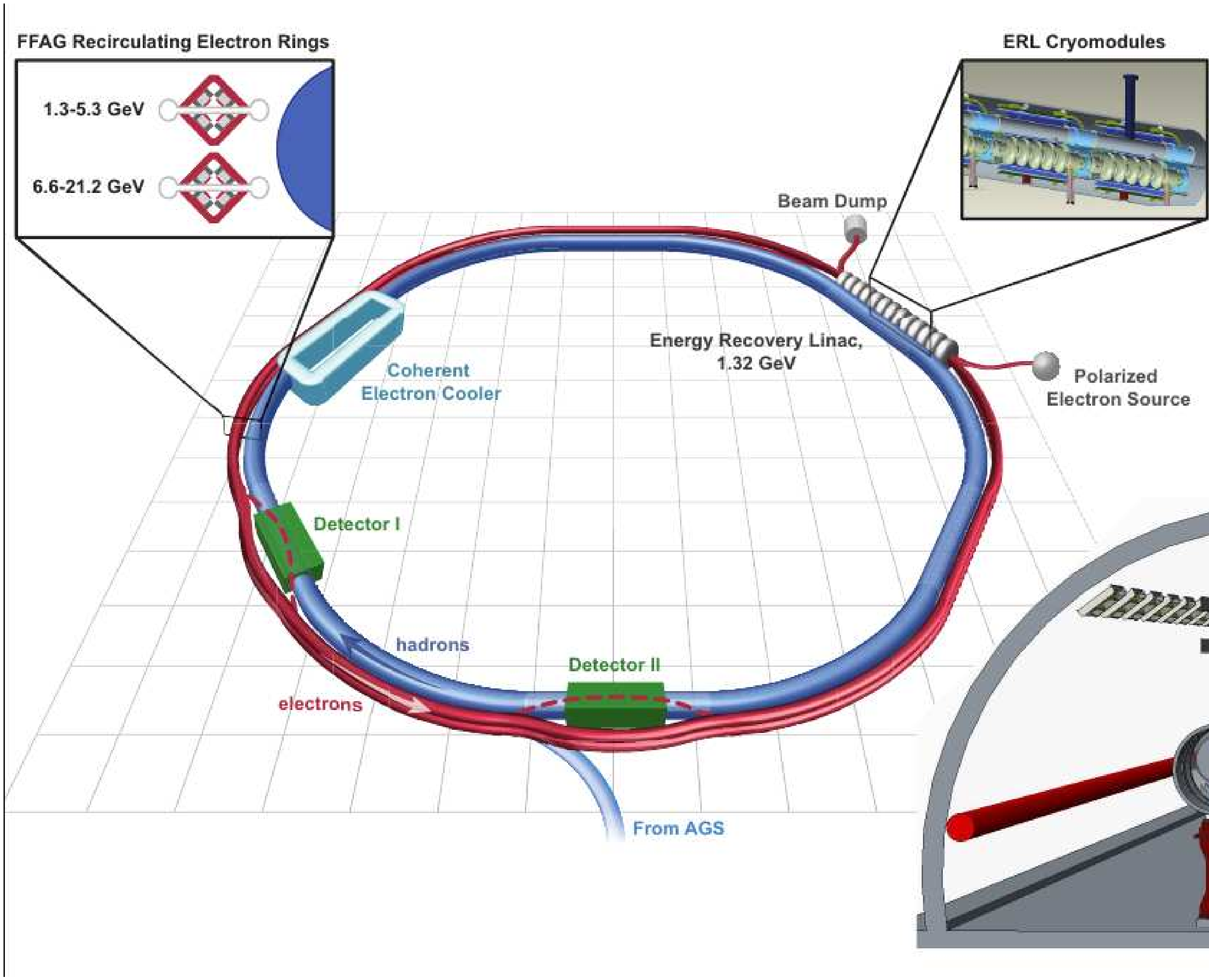

FFAG Recirculating Electron Rings
1.3-5.3 GeV
6.6-21.2 GeV
ERL Cryomodules
Beam Dump
Energy Recovery Linac, 1.32 GeV
Polarized Electron Source
Coherent Electron Cooler
Detector I
Detector II
hadrons
electrons
From AGS

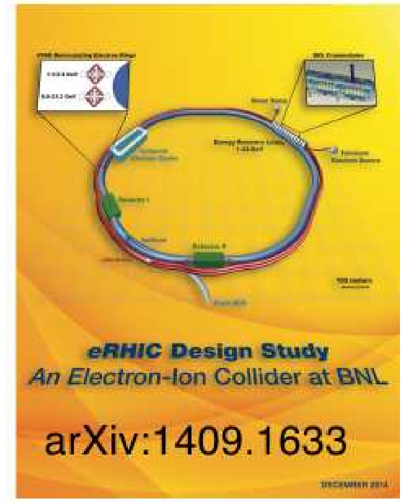

eRHIC Design Study
An Electron-Ion Collider at BNL
arXiv:1409.1633

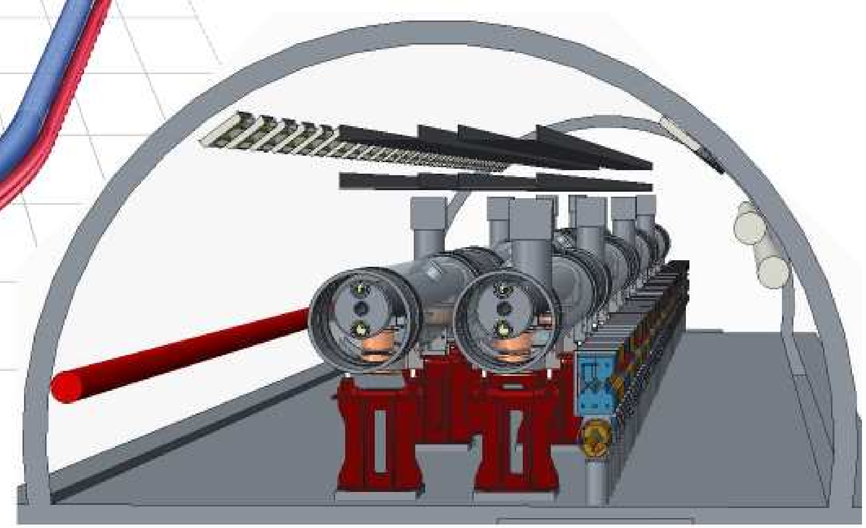

1 Basic principles

1.1 Particle dynamics

• **Electrons circulating in eRHIC FFAG arcs loose energy by synchrotron radiation (SR)**

Over a trajectory arc $\Delta\theta$, with constant curvature $1/\rho$, relative average energy loss :

$$\frac{\overline{\Delta E}}{E} = 1.879 \times 10^{-15}\,\frac{\gamma^3}{\rho}\,\Delta\theta$$

Energy loss at top energy, starting with E=21.16 GeV :

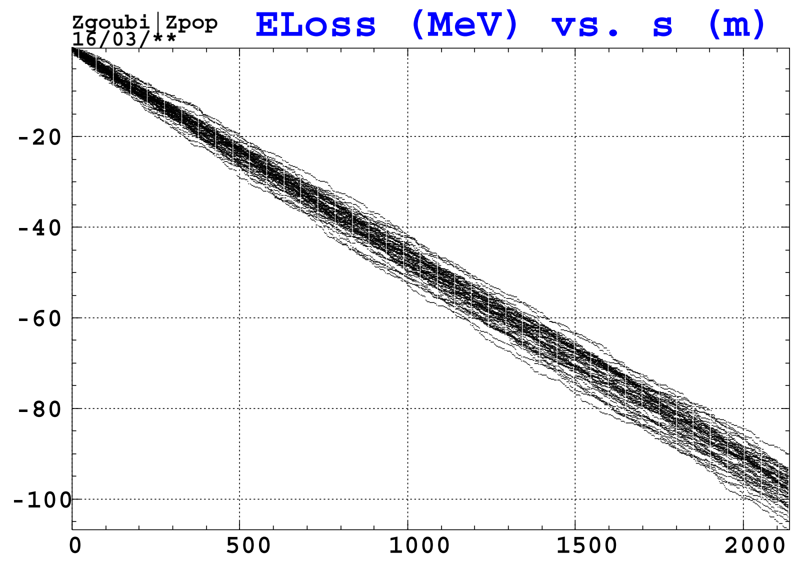

*** Ex. : at E=21.16 GeV, loss over a 6-arc ring, 2138 m distance, is $\boxed{\overline{\Delta E} \approx 100}$ MeV.**

• **SR is a stochastic process, photons fluctuate in number and energy, thus inducing**

- energy spread,

$$\frac{\sigma_E}{E} = 3.794 \times 10^{-14} \frac{\gamma^{5/2}}{\rho} \sqrt{\Delta\theta}$$

*** Ex. : $\boxed{\sigma_E = 5.2\ \mathbf{MeV}}$ after 11 passes in eRHIC from 7.94 to 21.16 GeV.**

Energy spread σ_E after 11 passes in eRHIC from 7.944 to 21.16 GeV :

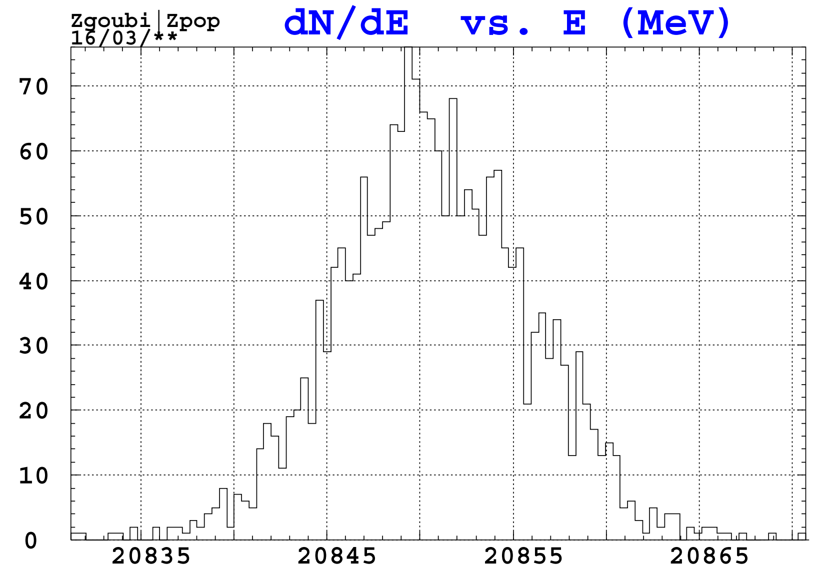

- and bunch lengthening [*],

$$\sigma_l = \left(\frac{\sigma_E}{E}\right) \left[\frac{1}{L_{\rm bend}} \int_s^{s_f} \left(D_x(s)T_{51}(s_f \leftarrow s) + D'_x(s)T_{52}(s_f \leftarrow s) - T_{56}\right)^2 ds\right]^{1/2}$$

(the integral is taken over the bends).

*** Ex. : bunch lengthening is $\boxed{\sigma_l \approx 5\ \mu\mathbf{m}}$ at 21.16 GeV in a 6-arc ring.**

---

[*] G. Leleux et al., Synchrotron Radiation Perturbations in Long Transport Lines, PAC 91.

• **The energy loss causes a spiraling of the beam centroid.**

Over a distance $[s_i, s_f]$ **:**

$$\left[\begin{array}{c}\overline{x(s_f)} \\ \overline{x'(s_f)}\end{array}\right] = T(s_f \leftarrow s_i) \times \left[\begin{array}{c}\overline{x(s_i)} \\ \overline{x'(s_i)}\end{array} + \frac{\sigma_E}{E}\left\{\begin{array}{c}< U > \\ < V >\end{array}\right\}\right]$$

$$\left[\begin{array}{c}U(s_e) \\ V(s_e)\end{array}\right] = \left[\begin{array}{c}D_x(s_i) - \int_{s_i}^{s_e} \frac{T_{12}(s \leftarrow s_i)}{\rho(s)} ds \\ D'_x(s_i) + \int_{s_i}^{s_e} \frac{T_{11}(s \leftarrow s_i)}{\rho(s)} ds\end{array}\right]$$

Inward spiraling of the electron beam at 21 GeV in a 6-arc ring

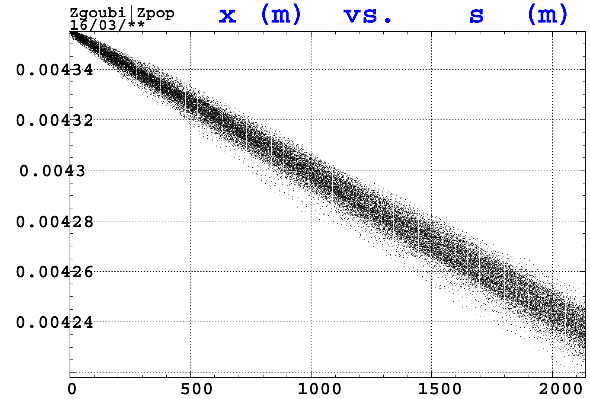

*** Ex. :** $\boxed{\Delta x = -0.12\,\mathrm{mm}}$ **at 21.16 GeV, over 6 arcs, 2138 m distance.**

• **and horizontal emittance growth,**

$$\Delta\sigma(s_f) = T(s_f \leftarrow s_i)\times$$

$$\left(\frac{\sigma_E}{E}\right)^2 \left[\begin{array}{cc}< U^2 > & < UV > \\ < UV > & < V^2 >\end{array}\right] \times \tilde{T}(s_f \leftarrow s_i)$$

Horizontal phase space after 21 passes 7.944 → 21.16 → 7.944 GeV.

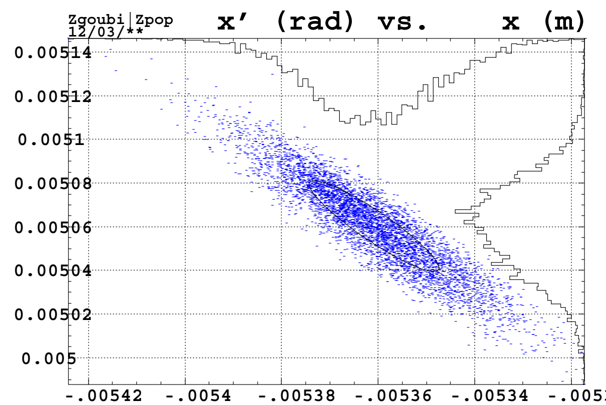

*** Ex. : SR induced emittance is** $\boxed{\beta\gamma\epsilon_x \approx 2\,\pi\mu\mathrm{m}}$**, after 11 passes in eRHIC, from 7.94 to 21.16 GeV.**

1.2 Spin

- **Averages and second momenta build up upon stochastic SR.**

- **Spin precession around the vertical dipole fields amounts to**

$$\phi = a\gamma\theta$$

$a = 1.1610^{-3}$, **anomalous gyromagnetic factor**

γ **is the Lorentz relativistic factor**

θ **is the particle deflection angle.**

*** Over a turn at E=21.16 GeV, spin undergoes $a\gamma$ ≈45 precessions around the vertical axis.**

- **Stochastic SR causes stochastic change in precession rate, hence spin diffusion**

Complete ERL ring, arcs+straights+DS. Starting 6-D emittance zero. Spin angle density after acceleration from 7.9 to 21.16 GeV in 11 passes :

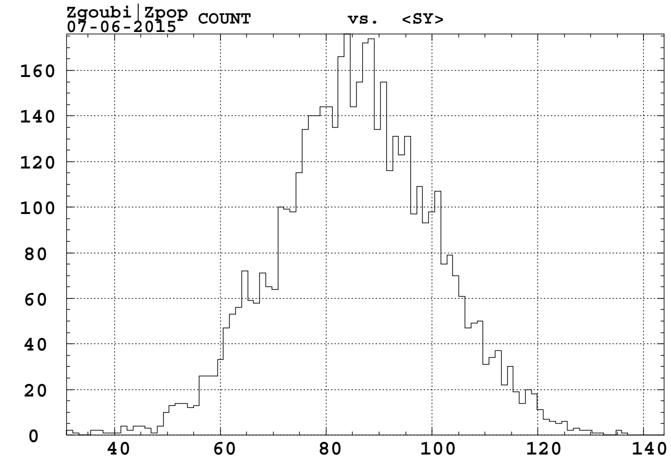

$\sigma_\phi = 14.89$ **deg**

$\cos(\sigma_\phi) = 0.966$

• **Evolution of the diffusion [*]**

In constant magnetic field : $$\begin{pmatrix} \overline{\Delta E^2} \\ \overline{\Delta E \Delta \phi} \\ \overline{\Delta \phi^2} \end{pmatrix} = \begin{pmatrix} 1 & 0 & 0 \\ \alpha s & 1 & 0 \\ \alpha^2 s^2 & 2\alpha s & 1 \end{pmatrix} \begin{pmatrix} \overline{\Delta E^2} \\ \overline{\Delta E \Delta \phi} \\ \overline{\Delta \phi^2} \end{pmatrix}_{s=0} + \omega \times \begin{pmatrix} s \\ \alpha s^2/2 \\ \alpha^2 s^3/3 \end{pmatrix}$$

$\omega = \frac{C}{\rho^3} \lambda\!\!\!^{-}_c r_e \gamma^5 E^2 \approx 1.44 \times 10^{-27} \frac{\gamma^5}{\rho^3} E^2$ **(**$\lambda\!\!\!^{-}_c = \hbar/m_e c$ **electron Compton wavelength, E in GeV),**
$C = 110\sqrt{3}/144$**,**
$\alpha = \frac{a}{\rho E_0} \approx \frac{1}{0.4406\rho}$ **(with** $a = 1.16 \times 10^{-3}$**, electron mass** $E_0 = 0.511 \times 10^{-3}$ **GeV).**

• **Cumulated spread, over a six-arc ring (2138 m circumference), from 7.9 to 21.2 GeV :**

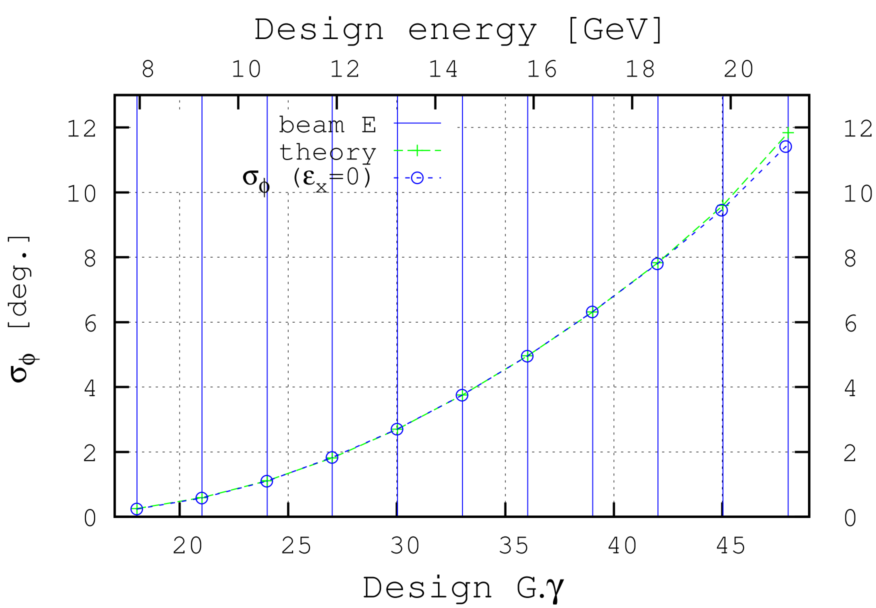

---

[*] cf. V. Ptitsyn, EIC'14

• Ray-tracing

Particle and spin motion

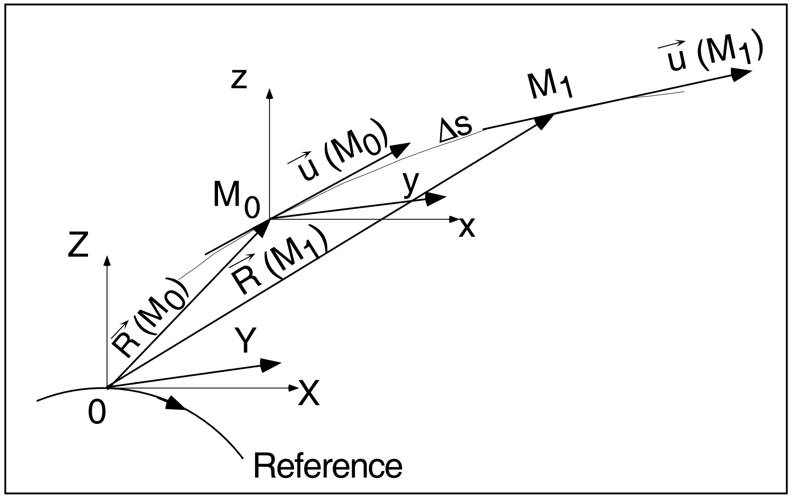

Position and velocity of a particle, pushed from location M_0 to location M_1 in Zgoubi frame.

$$\frac{d(m\vec{v})}{dt} = q\,(\vec{e} + \vec{v} \times \vec{b})\ ,$$

$$\frac{d\vec{S}}{dt} = \frac{q}{m}\,\vec{S} \times \vec{\omega}$$

with $\vec{\omega} = (1 + \gamma a)\vec{b} + a(1 - \gamma)\vec{b}_{/\!/}$

a : gyromagnetic factor, γ : Lorentz relativistic factor, c : velocity of light, q : charge, m :mass.

• Both equations are solved using a truncated Taylor series in the step size Δs,

$$\vec{a}(M_1) \approx \vec{a}(M_0) + \frac{d\vec{a}}{ds}(M_0)\,\Delta s + ... + \frac{d^n\vec{a}}{ds^n}(M_0)\,\frac{\Delta s^n}{n!} \tag{1}$$

- Solving particle motion : $\vec{a}$ stands for position $\vec{R}$ or normalized velocity $\vec{u} = \vec{v}/v$,
- Solving spin motion : $\vec{a}$ stands for the spin $\vec{S}$.

• The local magnetic field and its derivatives fully determine the coefficients $a^{(n)} = d^n a/ds^n$ in this Taylor series.

2 eRHIC FFAG optics

• **Stepwise methods allow detailed insight in the FFAG cell:**

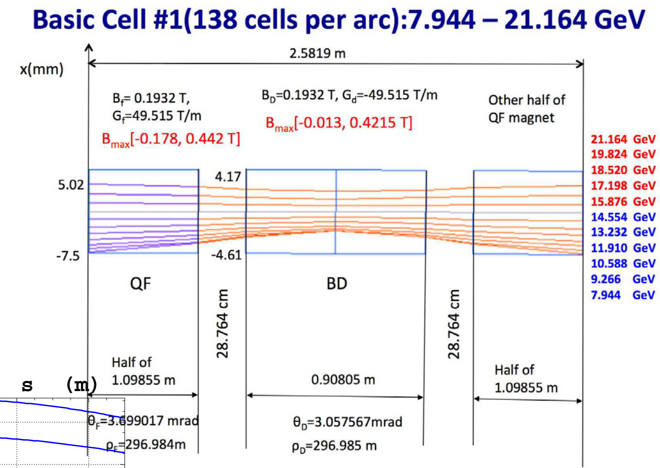

• **Orbits** in defocusing quad and focusing quad :

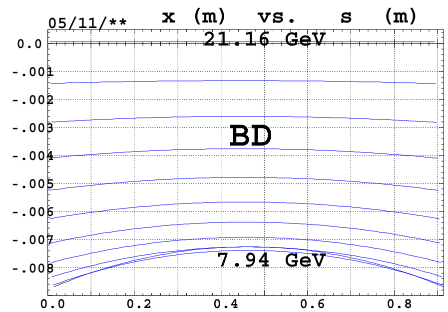

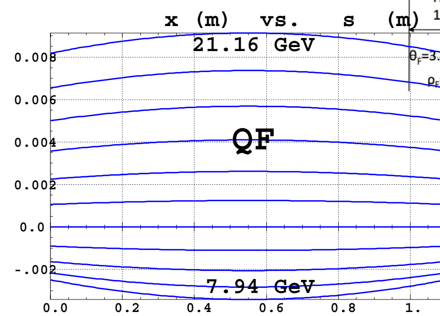

• **Field** along orbits :

Trajectory curvature varies continuously across the magnets.

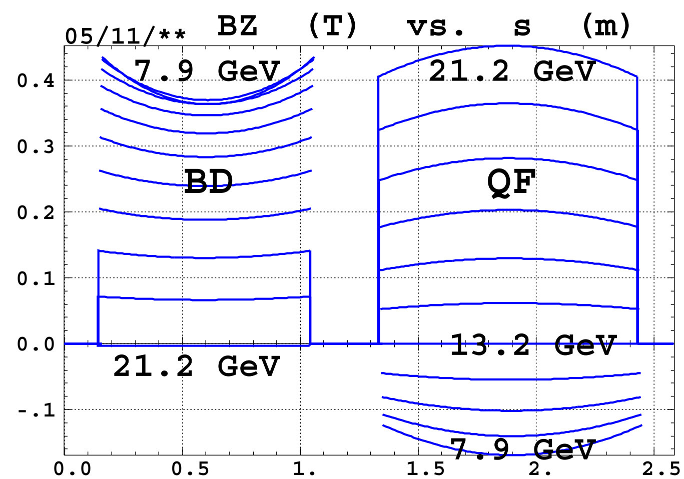

• **While we are here : hard edged magnet models will be used throughout, no such thing as "fringe fields", here.**

• **Cell : geometry, optics**

A continuous $a\gamma$ scan of the high energy FFAG eRHIC cell (7.944 → 21.16 GeV) :

Energy dependence of deviation and curvature radius in arc cell quads :

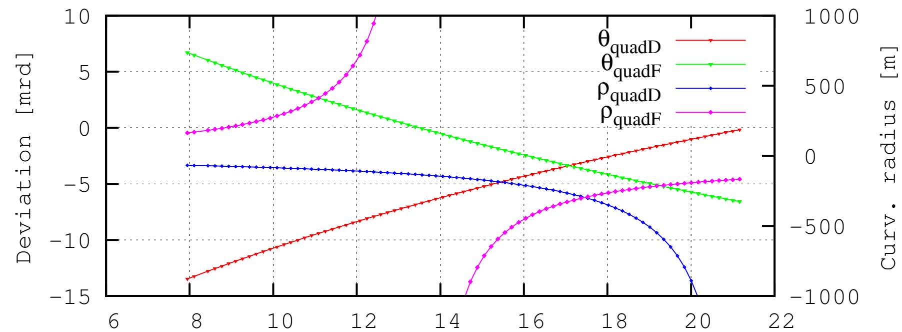

Cell tunes and chromaticities; the vertical bars materialize the 11 design energies :

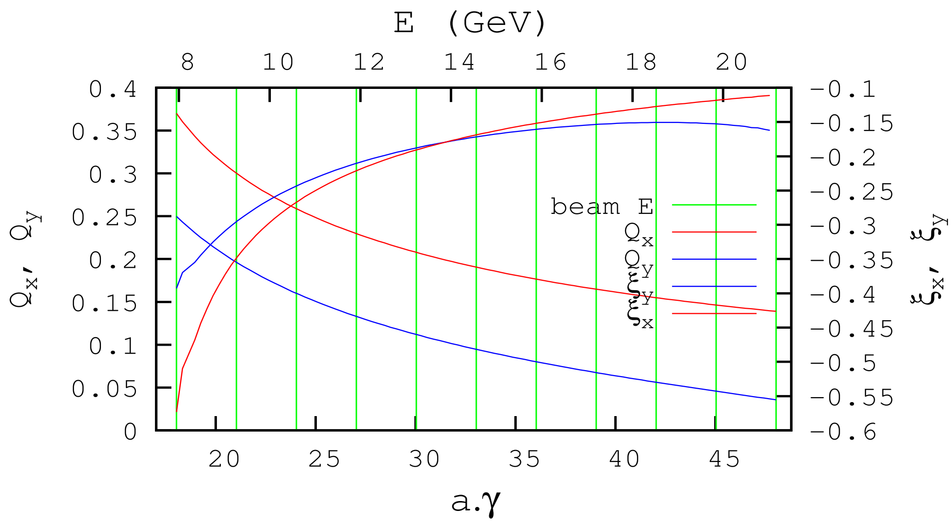

• **Matching polynomials can be devised :**

$$Q_x(a\gamma) = -0.002262268 + 8.60741/a\gamma - 120.24058/(a\gamma)^2 + 1545.2231/(a\gamma)^3$$

$$Q_y(a\gamma) = -0.140723255 + 11.113263/a\gamma - 153.6170/(a\gamma)^2 + 1457.3424/(a\gamma)^3$$

• **Note in passing : $a\gamma$ is close to an integer at all pass ⇐ linac kick multiple of mass/a=440.5MeV, for longitudinal alignment of polarization at IP6, IP8.**

- **More on optical functions**

SR induced ellipse mismatch, after one sextant at 21.16 GeV :

Horizontal phase-space, middle of drift, matched ellipses,
$E : 7.9 \rightarrow 21.2$ **GeV, step** 0.95 **GeV.**

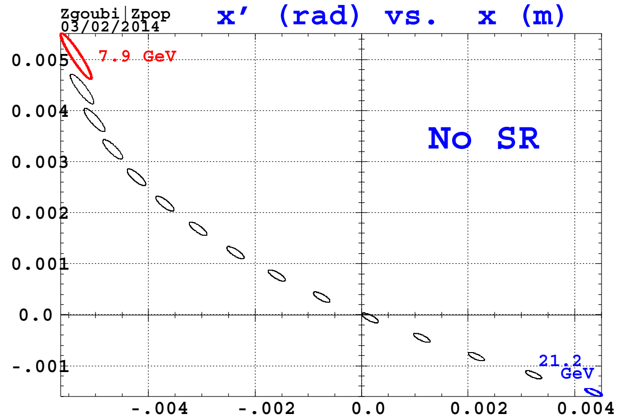

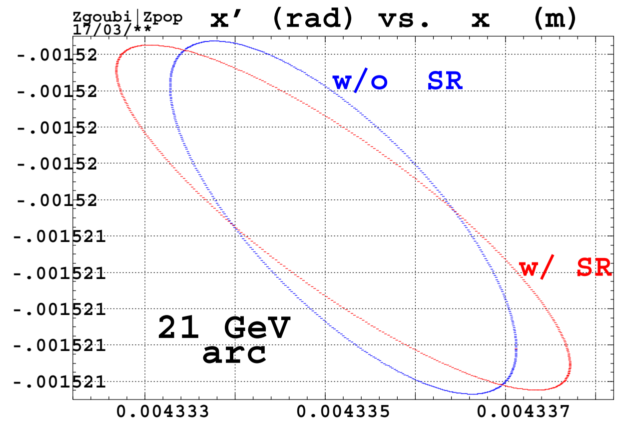

Middle of drift. Matched vertical ellipses,
$E : 7.9 \rightarrow 21.2$ **GeV, step** 0.14 **GeV.**

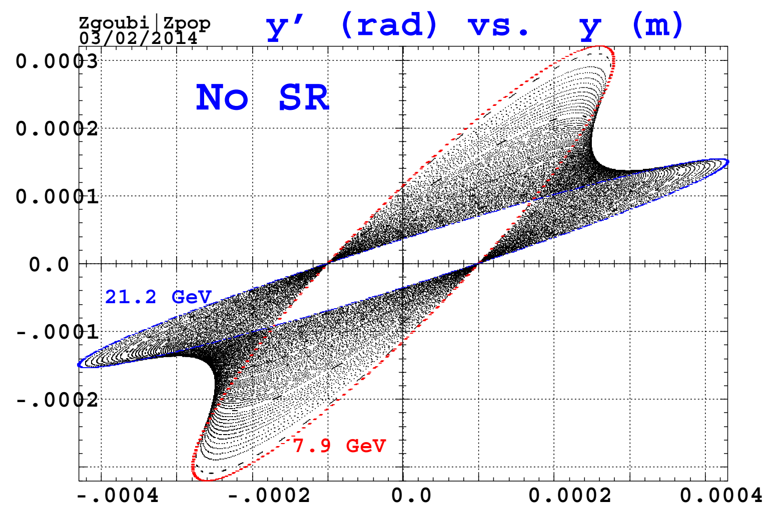

- **Tight comparisons have been performed between codes : SYNCH, MUON1, MADX[-PTC]. The conclusion is : good in general, some discrepancies are observed *(some may be serious)***

3 Dynamical effects of SR in eRHIC FFAG-II ERL

3.1 Working conditions

- **A complete FFAG-II ring ($7.944 \to 21.16$ GeV) is considered in the simulations discussed here.**

- **A ring is built from 6 arcs, 6 long straight sections (LSS), and 12 dispersion suppressors (DS)**

$$6 \times \left[\frac{1}{2}\text{LSS} - \text{DS} - \text{ARC} - \text{DS} - \frac{1}{2}\text{LSS}\right] + \textbf{Linac}$$

It includes one, zero-length, 1.322 GeV energy kick in a straight section (possibly accounting for phase), in order to simulate the linac.

- An arc is a series of FD 138 cells. The deviation is almost $2\pi/6$ ($2\pi/6.74$).

- A DS has 17 arc-type cells, but for vanishing quadrupole axis shift from arc to LSS

- An LSS is made of 70 such cells, with quadrupole axes aligned

- **The bunch to be tracked will in general be launched from the center of a long straight section,**

  - where theoretical local orbit has the virtue of being zero, whatever the bunch energy

  - with initial transverse/longitudinal emittances either zero or nominal, depending on the exercise

  - beam centroid is in general (artificially) re-centered on the LSS axis, at each LSS.

3.2 Orders of magnitude of the effects

3.2.1 Longitudinal phase space

• **Turn-by-turn energy loss and spread :**

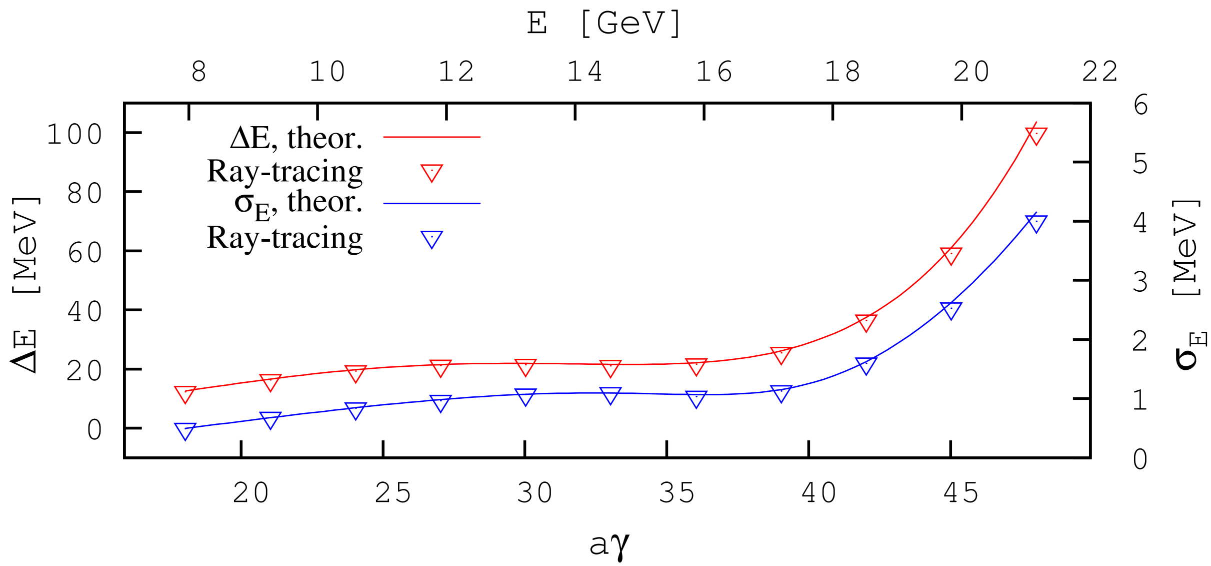

• **What is monitored here is energy density, average and spreading.**

Example, 5000 particles at end of pass #11 (21 GeV) :

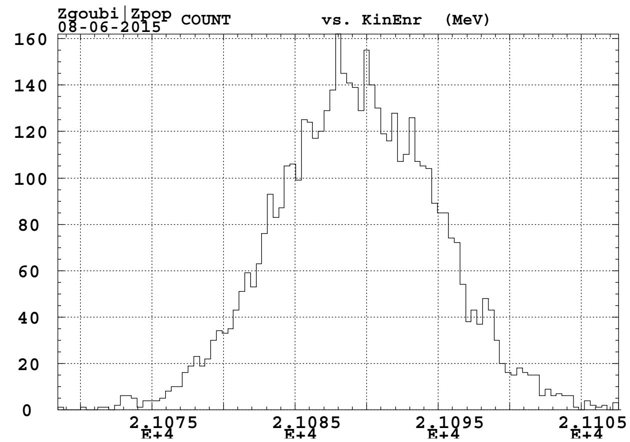

• **Approximation to** $\Delta E \propto E^2\, B^2 \Delta t$**, taking** $\overline{\rho_{\rm QF}} = l_{\rm QF}/\theta_{\rm QF}$**,** $\overline{\rho_{\rm BD}} = l_{\rm BD}/\theta_{\rm BD}$ **:**

$$\overline{\Delta E}[MeV] = \overline{\Delta E_{QF}} + \overline{\Delta E_{BD}} \approx 0.96\times 10^{-15}\gamma^4 \left(\frac{\theta_{\rm QF}}{|\overline{\rho_{\rm QF}}|} + \frac{\theta_{\rm BD}}{|\overline{\rho_{\rm BD}}|}\right) \quad \textbf{per} \quad \textbf{cell} \qquad (2)$$

• **Assuming** $< (1/\rho)^2 > \approx 1/\overline{\rho}^2$**, then :**

$$\sigma_E \approx \sqrt{\sigma^2_{E,{\rm QF}} + \sigma^2_{E,{\rm BD}}} \approx 1.94\times 10^{-14}\gamma^{7/2} \sqrt{\frac{\theta_{\rm QF}}{\overline{\rho_{\rm QF}}^2} + \frac{\theta_{\rm BD}}{\overline{\rho_{\rm BD}}^2}} \quad \textbf{per} \quad \textbf{cell} \qquad (3)$$

- **Bunch lengthening (still zero initial ϵ_x, ϵ_y and dp/p)**

Longitudinal bunch distribution at end of full 7.944 $\rightarrow$ 21.16 GeV cycle :
$\sigma_l = 0.11$ **mm.**

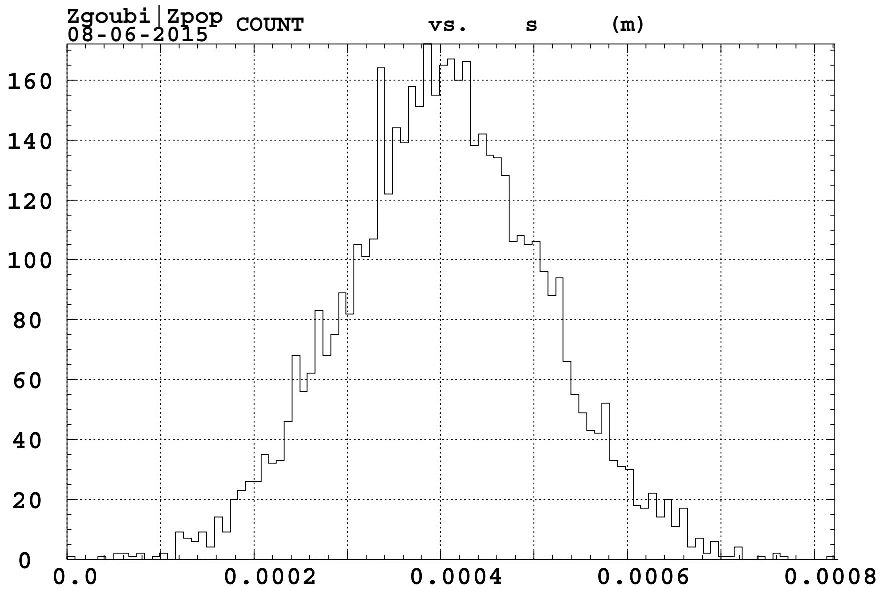

- **Bunch lengthening :** $\sigma_l = \left(\frac{\sigma_E}{E}\right) \left[\frac{1}{L_{\text{bend}}} \int_0^{L_{\text{bend}}} \left(D_x(s)T_{51}(s_f \leftarrow s) + D'_x(s)T_{52}(s_f \leftarrow s) - T_{56}\right)^2 ds\right]^{1/2}$

3.2.2 Transverse phase space

- **Energy loss causes drift of bunch centroid, stochasticity causes horizontal emittance increase.**

x-drift along the 6 arcs in eRHIC ring, at $E = 21.164$ GeV

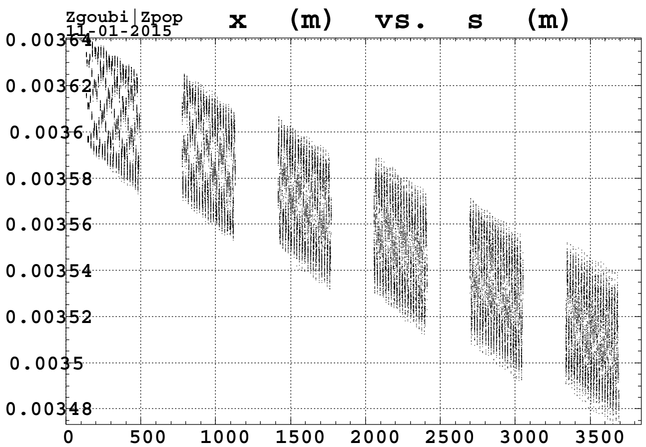

Horizontal phase space after the $E = 21.164$ GeV pass

$\overline{x_f} = -15\ \mu$m, $\sigma_{x_f} = 4.3\ \mu$m

$\overline{x'_f} = -1.1.\ \mu$rad, $\sigma_{x'_f} = 1.8\ \mu$rad.

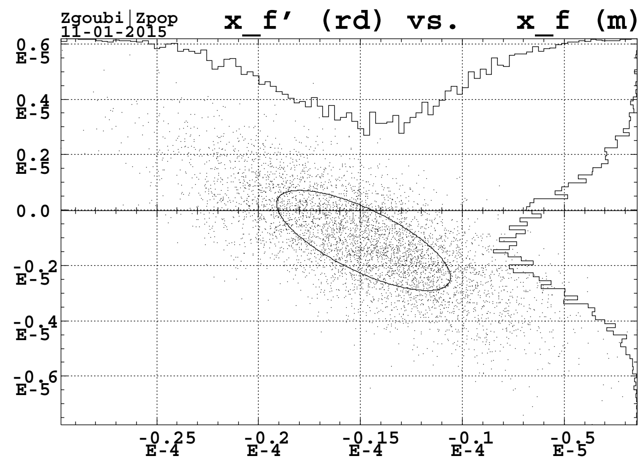

- **Beam centroid motion :**

$$\begin{bmatrix} \overline{x(s_f)} \\ \overline{x'(s_f)} \end{bmatrix} = T(s_f \leftarrow s_i) \times \left[\begin{Bmatrix} \overline{x(s_i)} \\ \overline{x'(s_i)} \end{Bmatrix} + \frac{\sigma_E}{E} \begin{Bmatrix} < U > \\ < V > \end{Bmatrix} \right] \quad \textbf{with} \quad \begin{bmatrix} U(s) \\ V(s) \end{bmatrix} = \begin{bmatrix} D_x(s_i) - \int_{s_i}^{s} \frac{T_{12}(s \leftarrow s_i)}{\rho(s)} ds \\ D'_x(s_i) + \int_{s_i}^{s} \frac{T_{11}(s \leftarrow s_i)}{\rho(s)} ds \end{bmatrix}$$

- **Perturbation of the beam matrix :** $\Delta\sigma(s_f) = T(s_f \leftarrow s_i)\, 4 \left(\frac{\sigma_E}{E}\right)^2 \begin{bmatrix} < U^2 > & < UV > \\ < UV > & < V^2 > \end{bmatrix} \times \tilde{T}(s_f \leftarrow s_i)$ (4)

3.3 End-to-end bunch tracking, cumulated effects (initial $\epsilon_x \approx \epsilon_y = 0$ and dp/p=0)

Qualitatively, orbits in arcs, pass 1 to 21 :

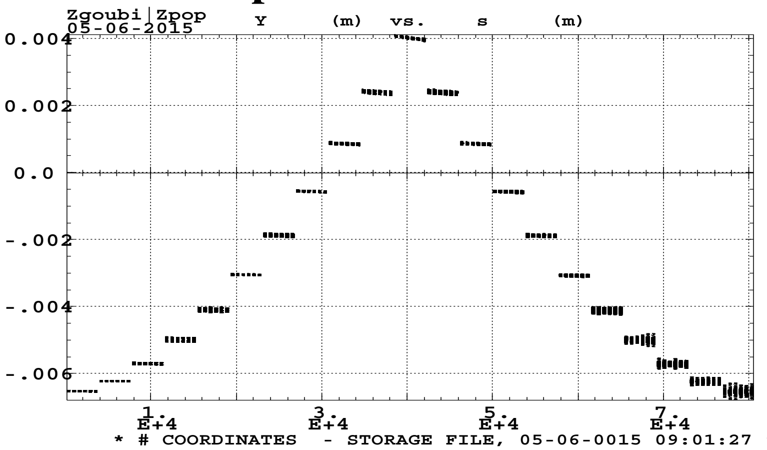

(x,x') phase space, at 8, 10.6, 12 and 21 GeV (end of pass # 1, 3, 4, 11)

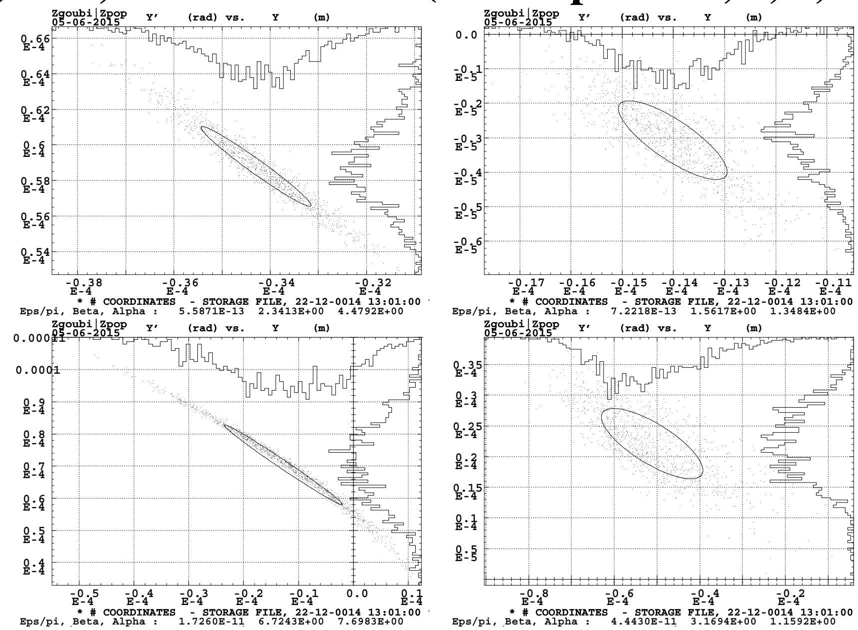

- **Note : the source of the orbit error that triggers the apparent emittance increase, due to the strong chromaticity, is the residual steering of the adiabatic DS.**

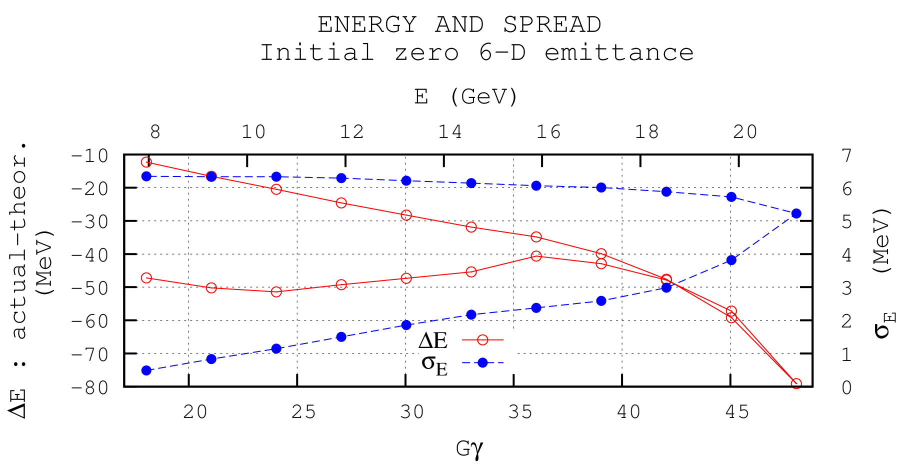

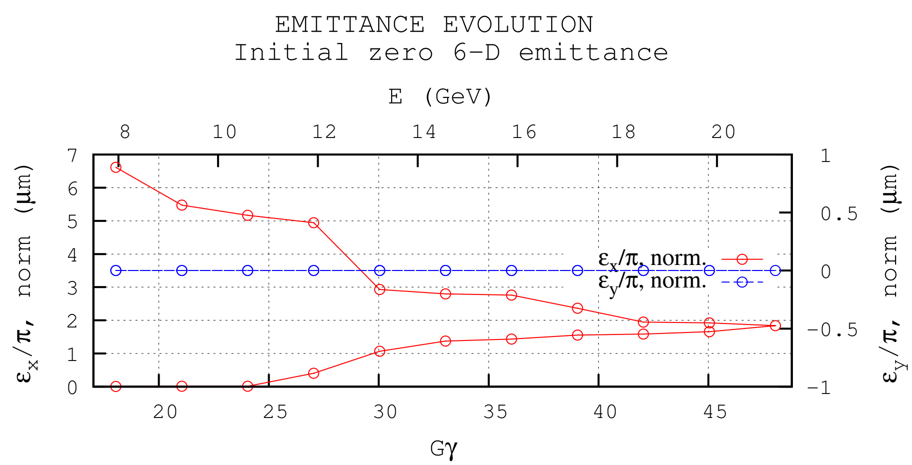

• **Evolution of the polarization**

Case initial ϵ_x, ϵ_y and dp/p_0 all zero

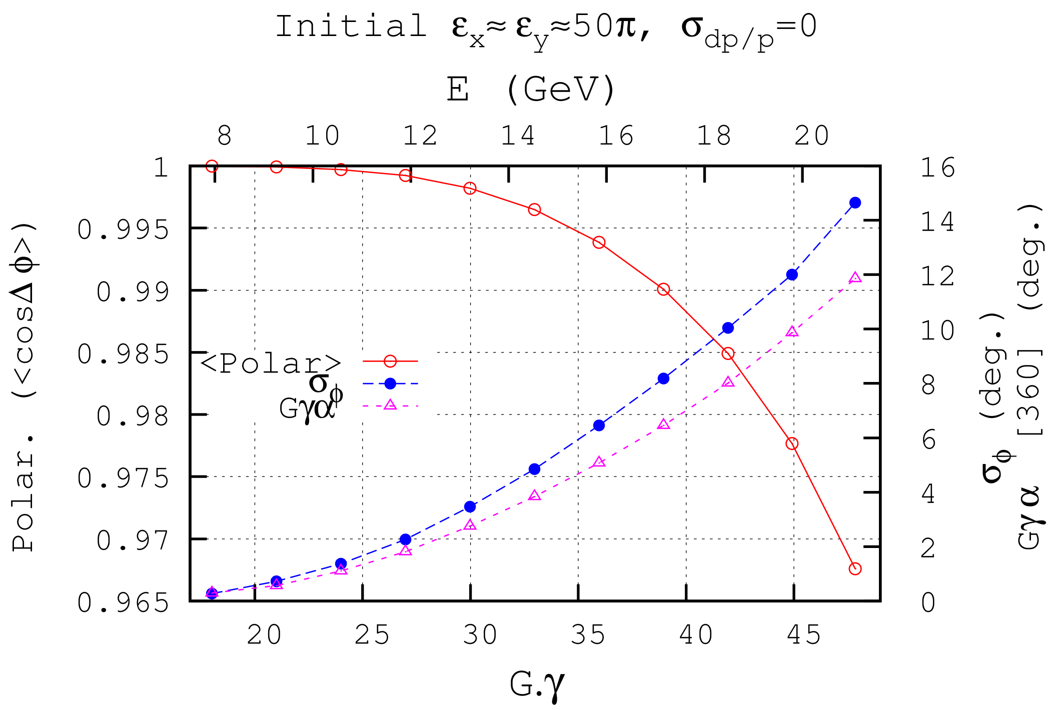

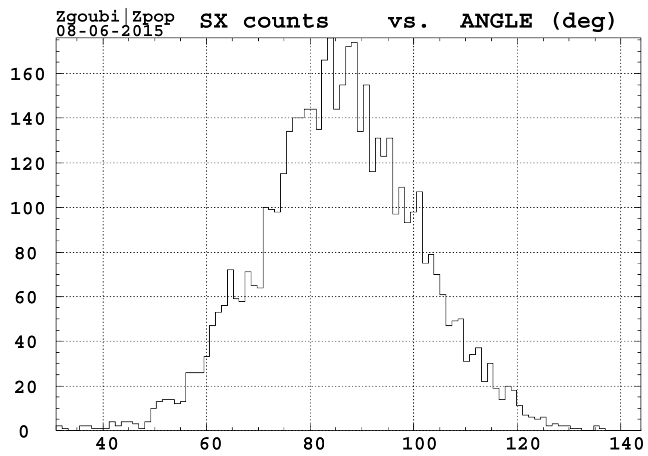

Density of horizontal spin component S_x at end of pass 11

$\sigma_\phi = 14.9$ **deg.**

3.4 End-to-end 9-D tracking, nominal initial transverse emittances $50\pi\mu$m

Case initial dp/p=0

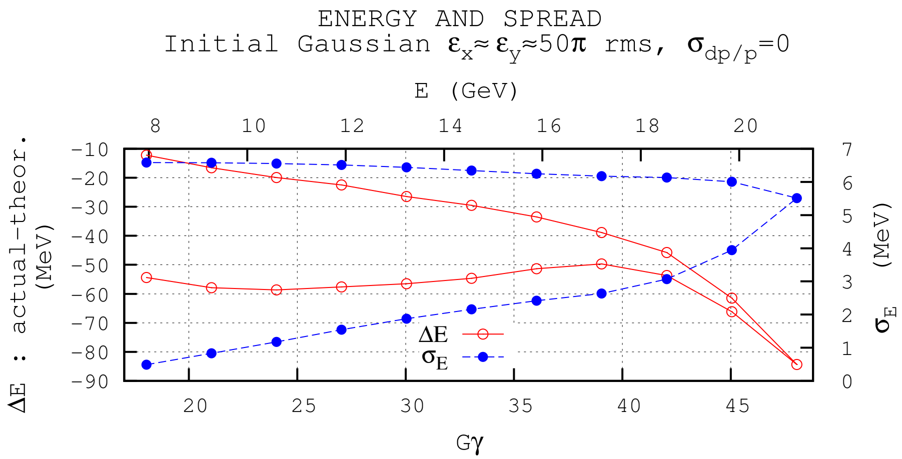

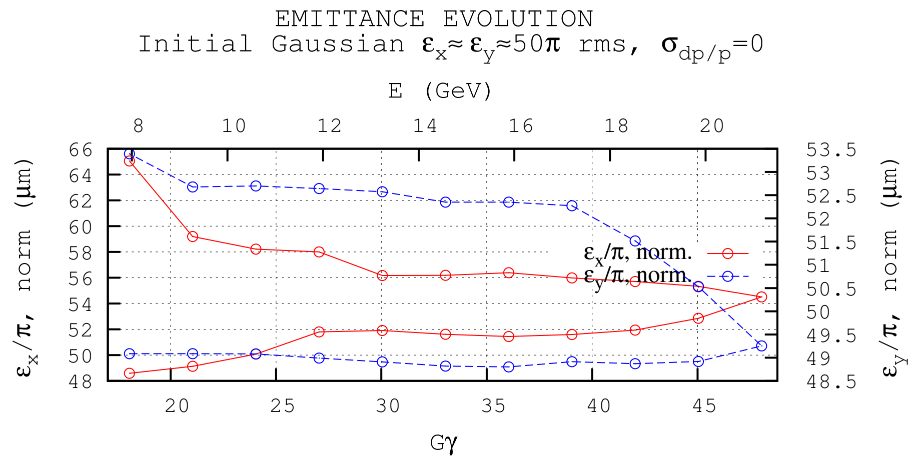

Case initial $dp/p_0 \in [-3, +3] \times 10^{-4}$

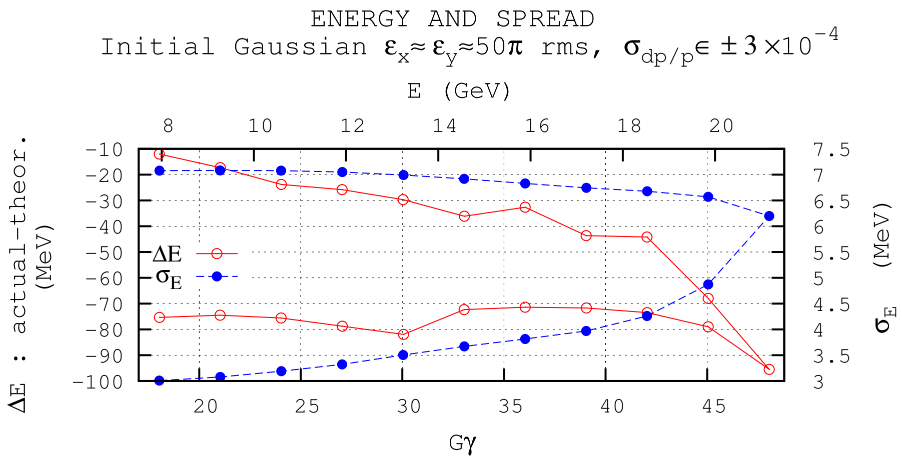

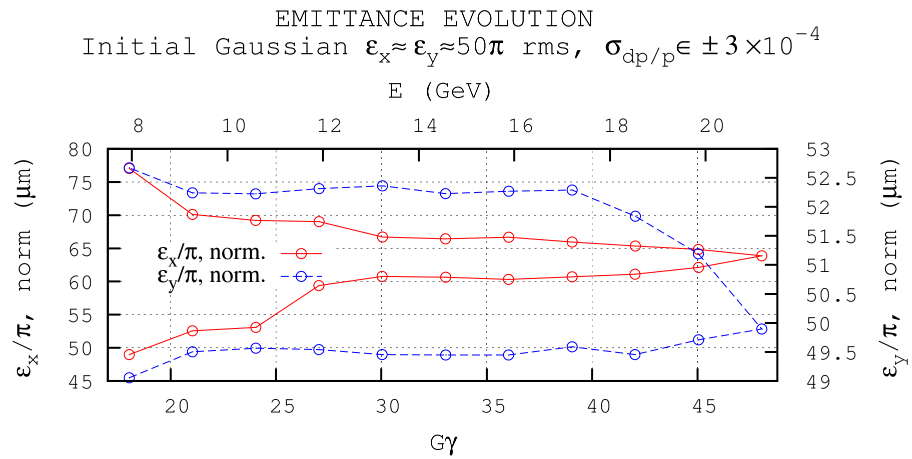

Polarization

Case initial $\epsilon_x \approx \epsilon_y \approx 50\,\pi$mm.mrad and $dp/p_0 = 0$

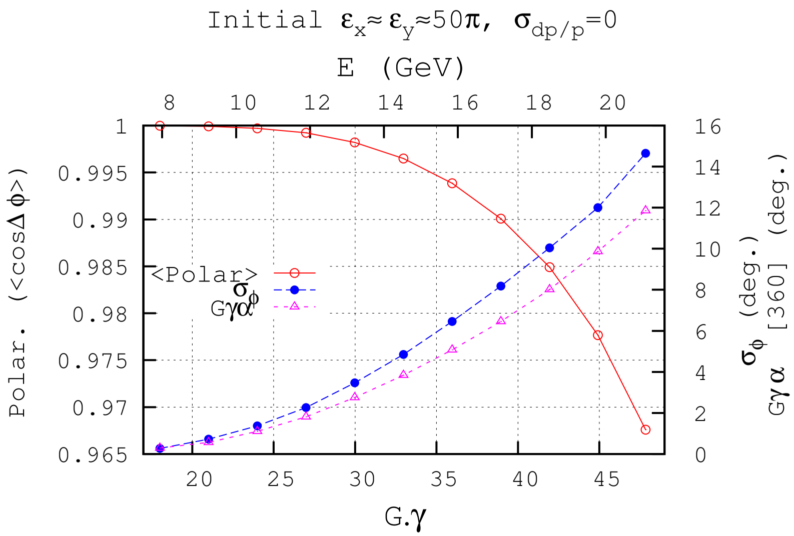

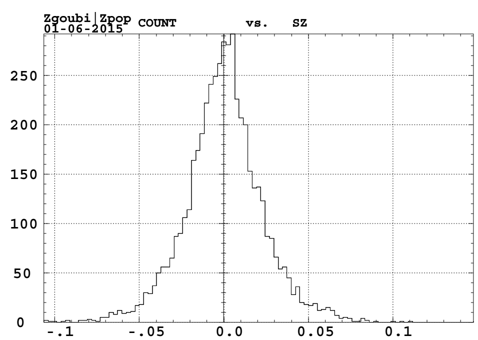

Vertical component of spin at end of pass 11 (end of pass 11 is 2 IPs beyond IP6 :

Avrg.	Sigma
6.304E-05	2.331E-02

Asin$(\sigma_{S_Z}) \approx 1.3$ **deg.**

Case initial $\epsilon_x \approx \epsilon_y \approx 50\,\pi$mm.mrad and $dp/p_0 \in \pm 3 \times 10^{-4}$

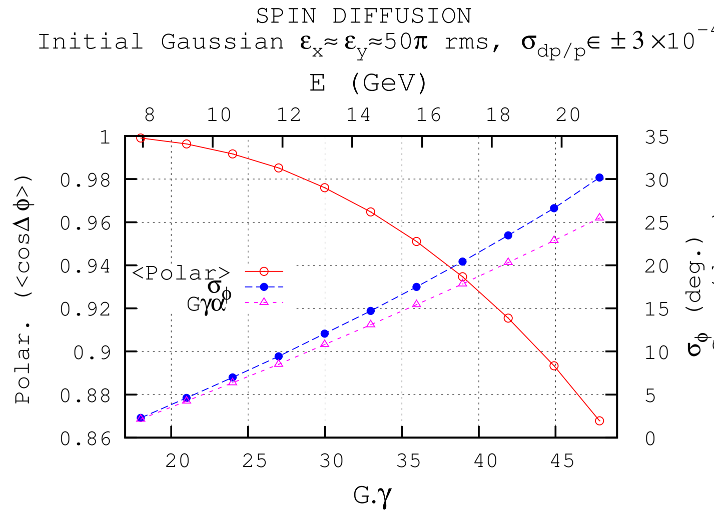

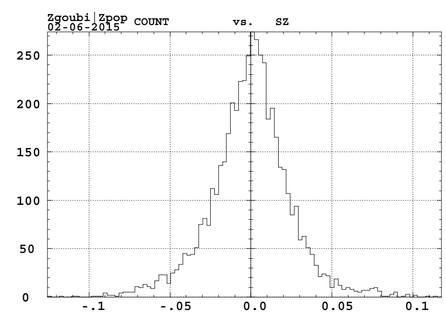

Vertical component of spin at end of pass 11 (end of pass 11 is 2 IPs beyond IP6 :

Avrg.	Sigma
-4.207E-04	2.495E-02

Asin$(\sigma_{S_Z}) \approx 1.43$ **deg.**

4 Dispersion suppressors

• The dispersion suppressors are based on a "missing magnet" style scheme, where the relative displacement of the two cell quadrupoles (the origin of the dipole effect in the FFAG cell) is brought to zero over a series of cells.

• From orbit viewpoint, a quadrupole displacement is equivalent to a kick θ_k at entrance and exit.

• Due to the varying displacement of the quads (from their misalignement in the arc to aligned configuration in the straight) the orbit builds along the DS (with origin at upstream arc, end at downstream straight, or reverse) following

$$\begin{cases} \frac{y_{\rm orb}(s)}{\sqrt{\beta(s)}} = \frac{y_{\rm orb}(0)}{\sqrt{\beta(0)}}\cos(\phi) + \frac{\alpha(0)y_{\rm orb}(0)+\beta(0)y'_{\rm orb}(0)}{\sqrt{\beta(0)}}\sin(\phi) + \sum_k \sqrt{\beta(s_k)}\theta_k \sin(\phi-\phi_k) \\ \frac{\alpha(s)y_{\rm orb}(s)+\beta(s)y'_{\rm orb}(s)}{\sqrt{\beta(s)}} = -\frac{y_{\rm orb}(0)}{\sqrt{\beta(0)}}\sin(\phi) + \frac{\alpha(0)y_{\rm orb}(0)+\beta(0)y'_{\rm orb}(0)}{\sqrt{\beta(0)}}\cos(\phi) + \sum_k \sqrt{\beta(s_k)}\theta_k \cos(\phi-\phi_k) \end{cases}$$

• Case of the 11.9GeV pass. The orbit is shown from end of first LSS to upstream region of first arc.

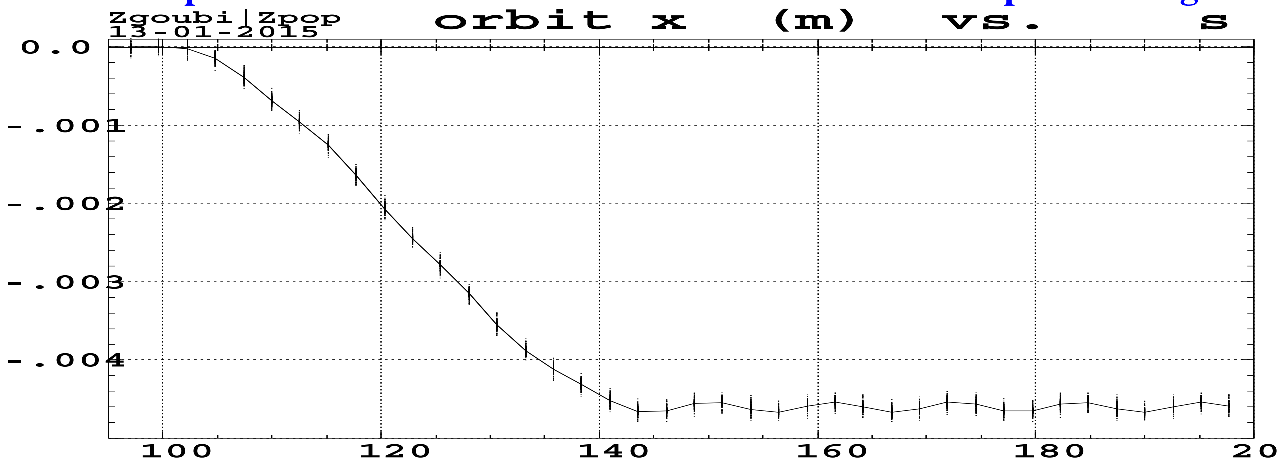

• However, the orbit build-up from LLS to arc ends up, at the arc, with (x,x') coordinates which do not *fully* coincide with the periodic orbit of the arc FFAG cell.

- **The orbit build-up depends on the phase advance $\phi = \int_0^s \frac{ds}{\beta(s)}$. Thus it depends on the cell tune, and on energy.**

Orbit along 5 ring-turns,
7.9, 9.3, 10.6, 11.9GeV and 13.2 GeV.

In each case starting coordinates are (x,x')=(0,0) at the center of an LSS.

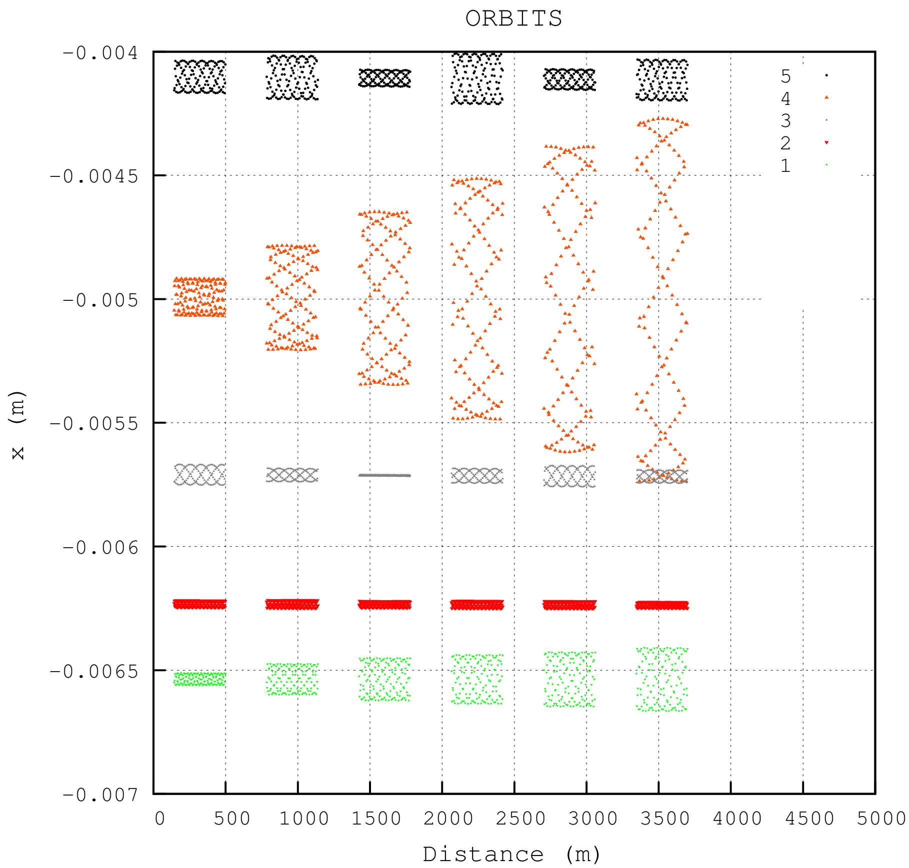

The orbit amplification is tune-dependent. For instance, case of pass #4:

Varied energy $\pm 1,\ 2,\ 3\%$ in the vicinity of $E = 11.9$GeV:

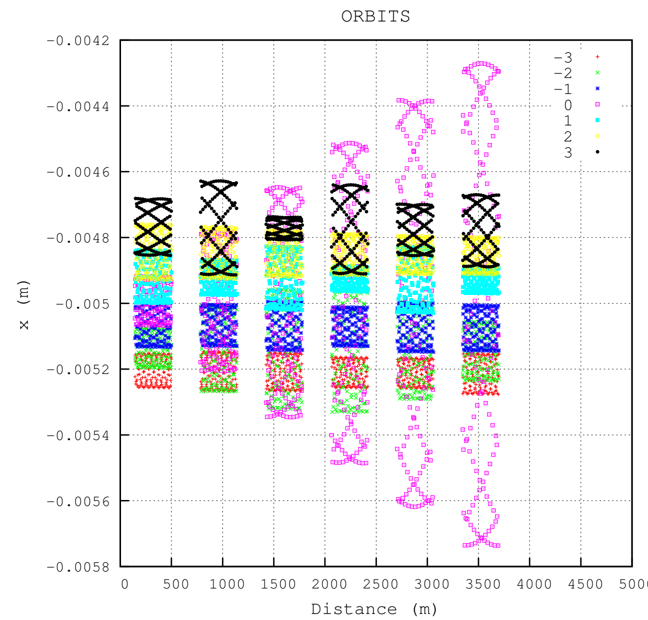

5 Dynamical acceptance of eRHIC FFAG lattice

Simulation conditions

• The available aperture at entrance to a pass around the ring is evaluated, independently for each one of the 11 energies in the range $7.944 : 21.164 : 1.322$**.**

• Two types of lattices are simulated, for comparison :

- either a single cell, ≈ 1000 **passes, this would be the dynamical acceptance at entrance into a 6-arc ring, 138 cells per arc**

- eRHIC ring acceptance window, observed at the center of a LSS.

$$\textbf{RING} = 6 \times \left[\frac{1}{2}\mathrm{LSS} - \mathrm{DS} - \mathrm{ARC} - \mathrm{DS} - \frac{1}{2}\mathrm{LSS}\right]$$

• The effects of some field defects are summarily investigated.

• There is no SR in these tracking, just geometrical effects are addressed (apart from all 11 energies being investigated).

SR increases beam emittance and is expected to decrease the dynamical acceptance accordingly.

- 1000-cell DA, hard-edge (left) and soft-edge (right)

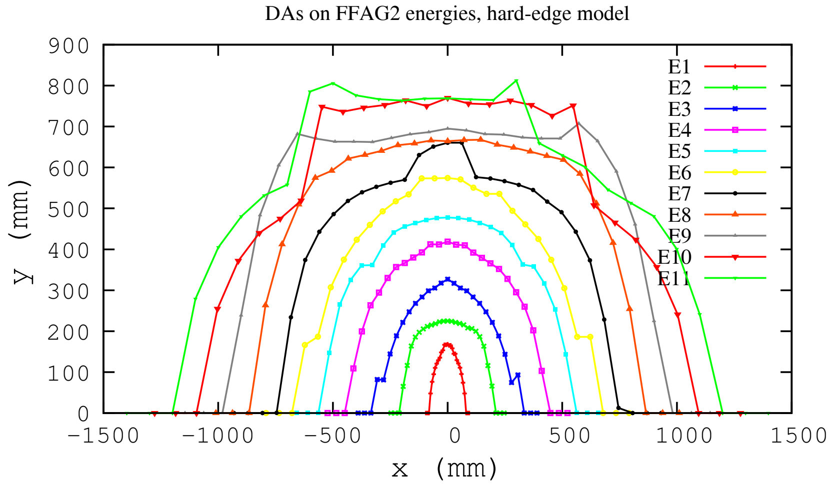

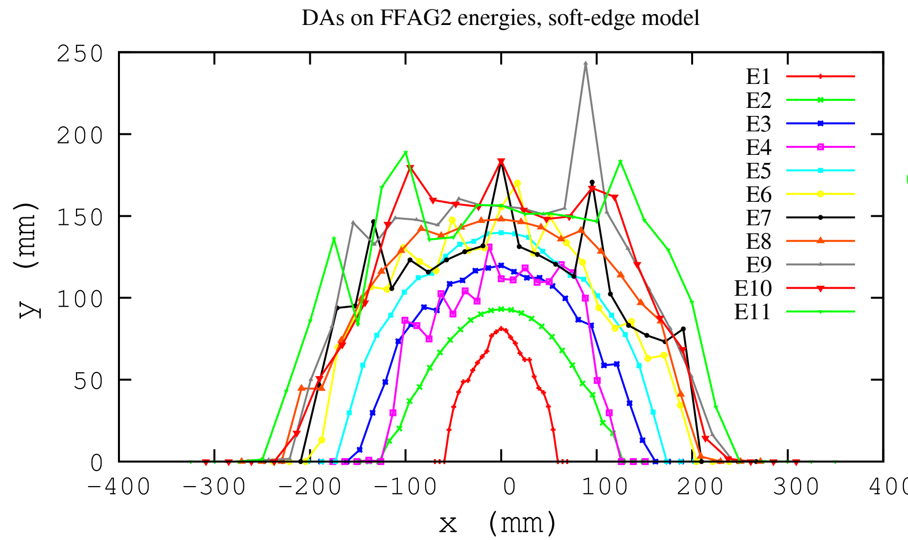

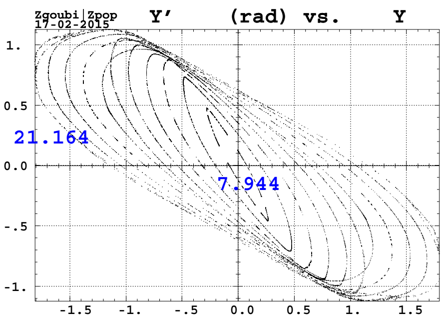

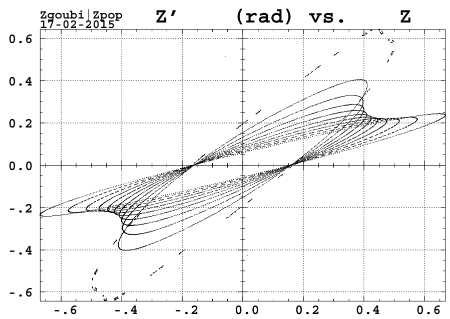

Maximum H (left) and V (right) invariants, 11 energies.

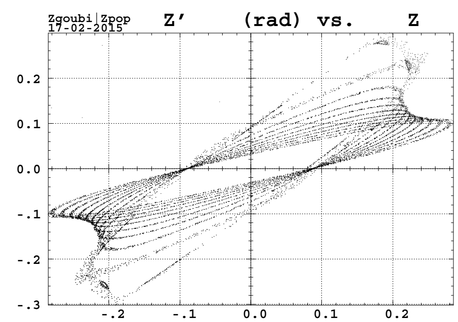

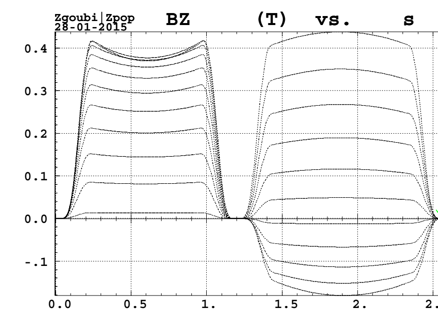

Maximum vertical invariants, 11 energies.
Fringe field model (after H. Enge) :

$$V(X,Y,Z) = \left(G - \frac{G''}{12}(Y^2+Z^2) + \frac{G''''}{384}(Y^2+Z^2)^2 - \frac{G''''''}{23040}(Y^2+Z^2)^3\right)Y$$

$$G(s) = \frac{G_0}{1+\exp P(s)} \quad \textbf{with} \quad G_0 = \frac{B_0}{R_0}$$

$$P(s) = C_0 + C_1\left(\frac{s}{\lambda}\right) + C_2\left(\frac{s}{\lambda}\right)^2 + C_3\left(\frac{s}{\lambda}\right)^3 + C_4\left(\frac{s}{\lambda}\right)^4 + C_5\left(\frac{s}{\lambda}\right)^5$$

Field along BD

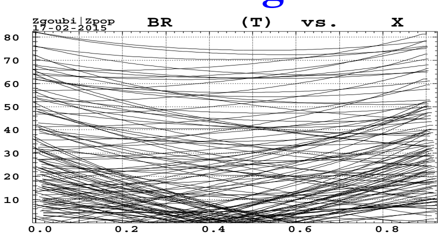

field along QF

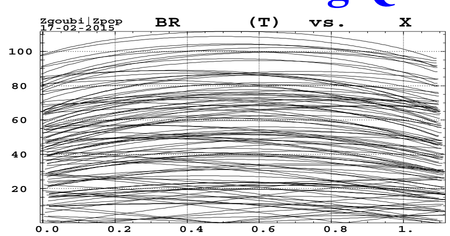

Smooth fields experienced by the 11 particles across the two cell quadrupoles

- 1000-cell DA, including dodecapole defect, random (top) and systematic (bottom)

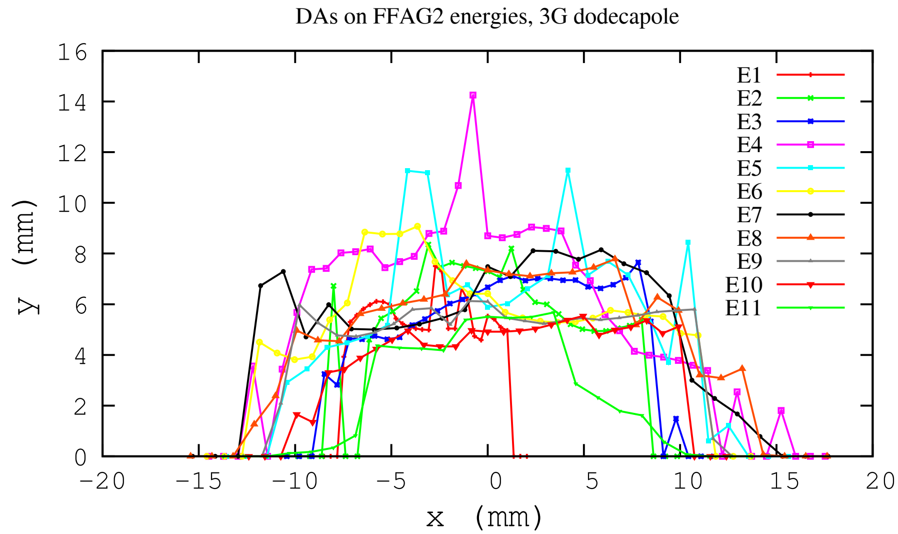

With random dodecapole defect,
± 3 Gauss at r=1 cm, uniform.

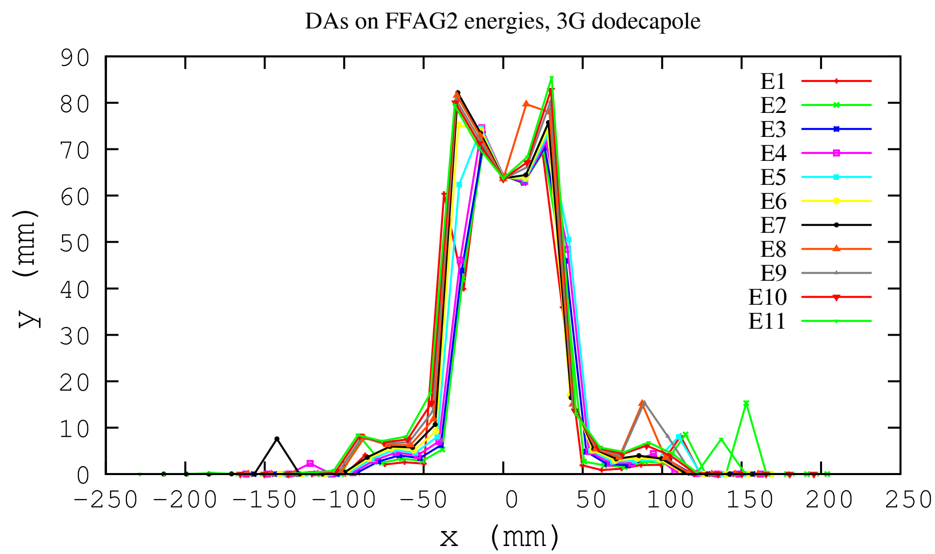

With systematic dodecapole defect
$+3$ Gauss at r=1 cm.

- **eRHIC ring, available aperture into the ring as seen at middle of LSS**

$$6 \times \left[\frac{1}{2}\mathrm{LSS} - \mathrm{DS} - \mathrm{ARC} - \mathrm{DS} - \frac{1}{2}\mathrm{LSS}\right]$$

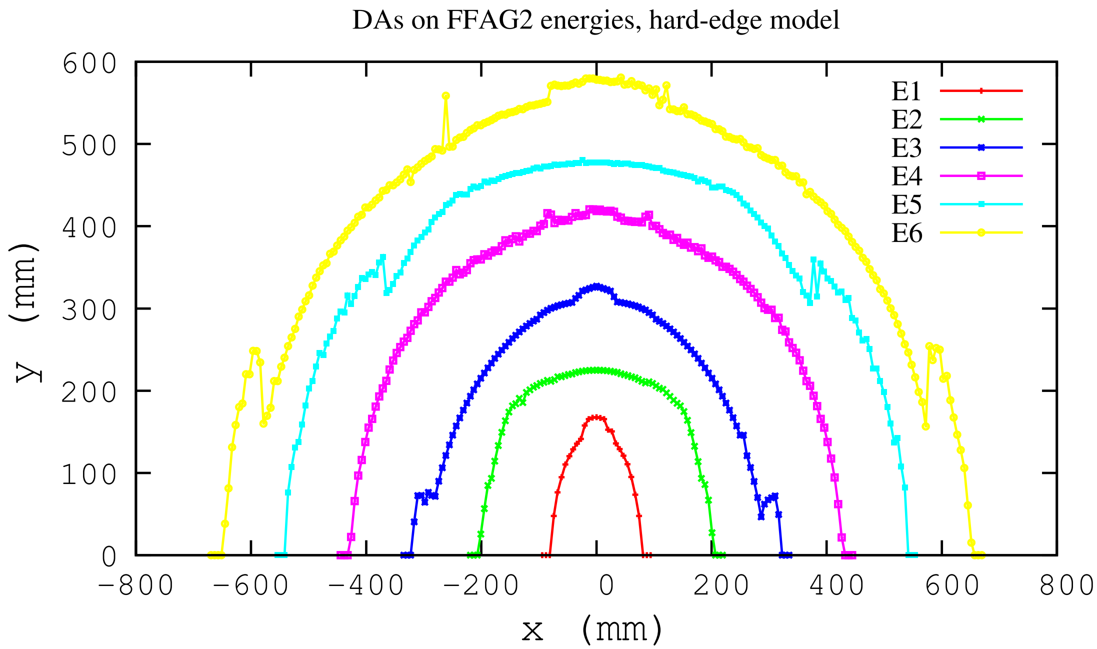

Available dynamic admittance of the ring, for 6 energies [7.944:21.164:2.644], observed at the center of an LSS, defect-free lattice.

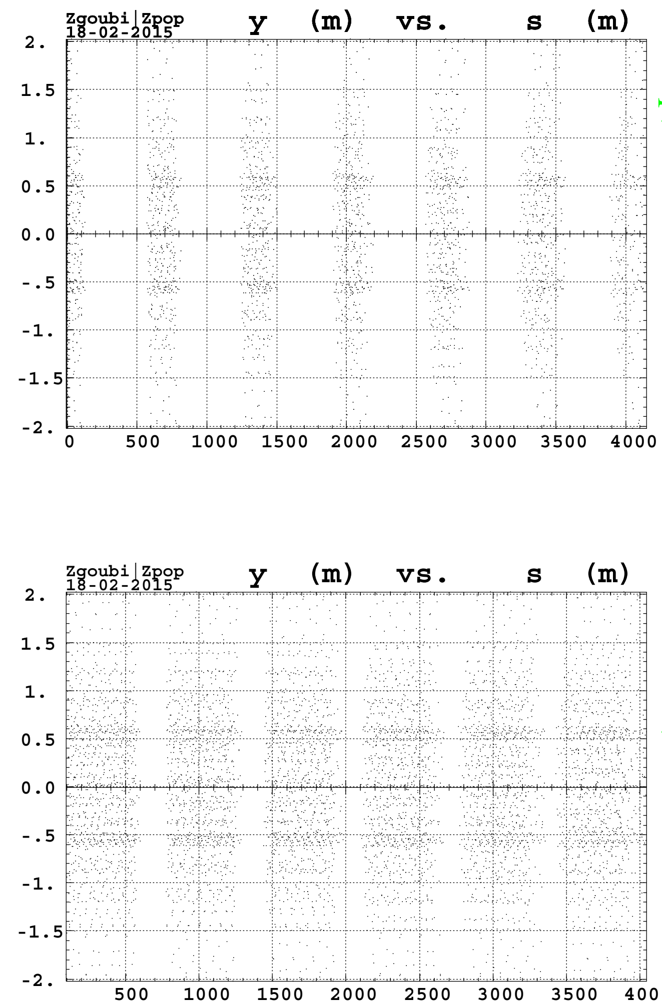

Vertical excursion along the 6 LSS (top) and 6 arcs (bottom), 6 particles (6 energies) launched at (x=0,y=max.).

- **eRHIC ring, available aperture into the ring as seen at middle of LSS, with dodecapole defect**

$$6 \times \left[\frac{1}{2}\mathrm{LSS} - \mathrm{DS} - \mathrm{ARC} - \mathrm{DS} - \frac{1}{2}\mathrm{LSS}\right]$$

Defect value retained here, following from prior study of emittance growth over single ring turn : ± 3 **Gauss at 1 cm (**$\pm 3G/5kG = 6 \times 10^{-4}$ **relative).**

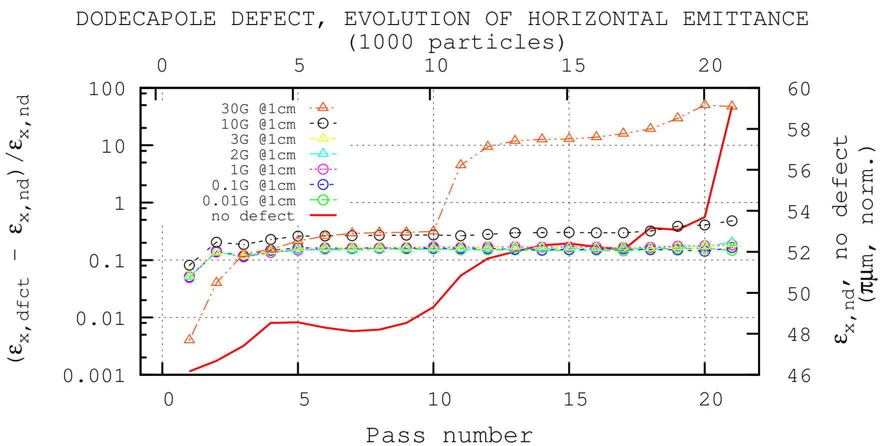

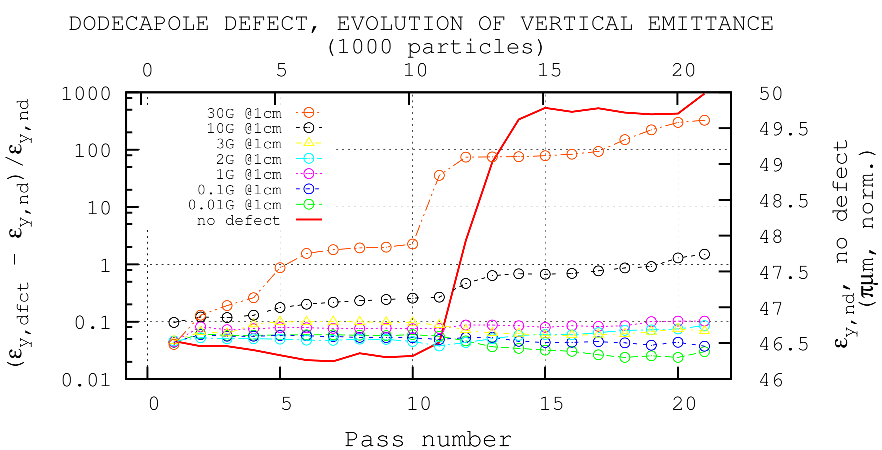

Hyp. in these two graphs : bunch centroid is re-centered (average position and angle are zero-ed) at entrance to each one of the 6 LSS.

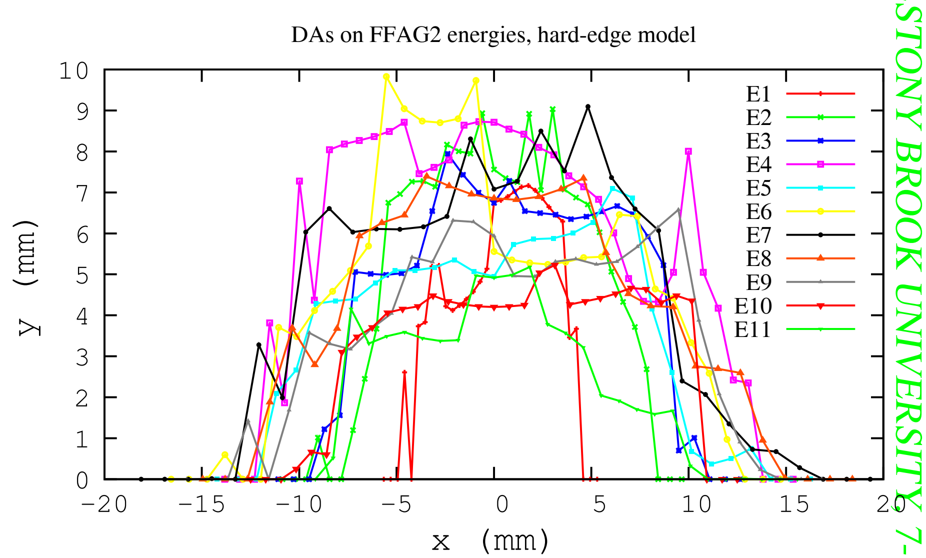

In the presence of dodecapole defect, ± 3 **G at 1cm, uniform available dynamic admittance of the ring, for 11 energies [7.944:21.164:1.322], Observation point is at the center of an LSS, where all orbits have a common reference axis.**

6 Injecting alignment defects

6.1 Horizontal misalignment

- An either 0, or 1, or 10 Gauss dipole defect is considered - random, uniform, applied to all quads around the ring
- **Qualitatively, below : 4 particles launched with initial $\epsilon_x = 0$ and $dp/p = 0$ (subject to increase due to SR) and initial $\epsilon_y = 50\pi\mu$m norm.**

Horizontal orbit excursion along the arcs (regions spanning large Δx values), and along the straights (regions with Δx values in the vicinity of x=0)

Vertical excursion around the ring, over the 21 passes :

db = zero

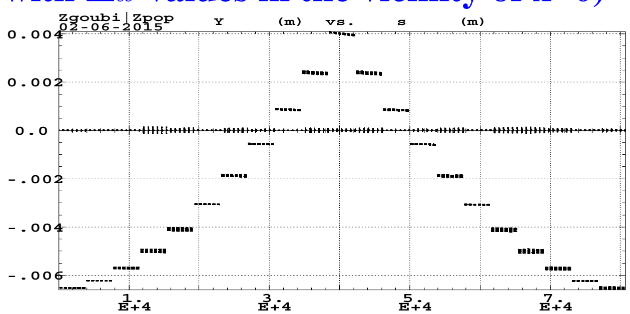

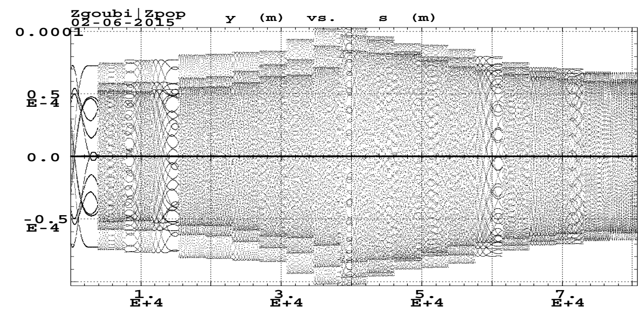

db = 1 G

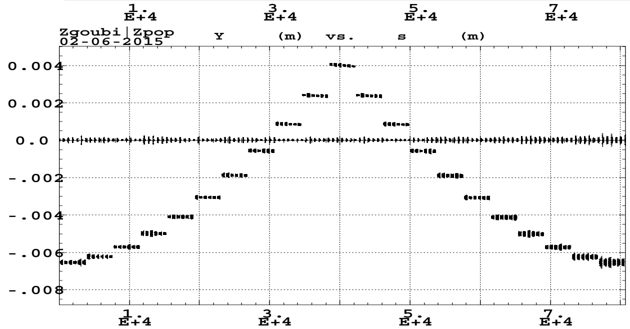

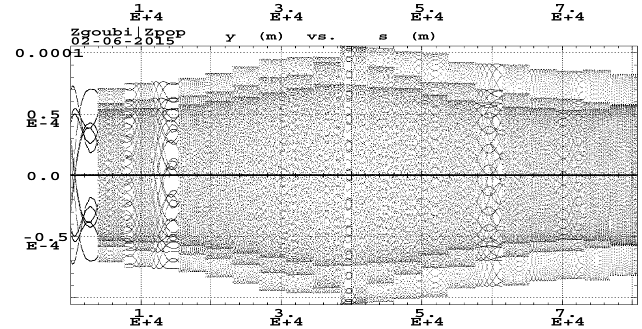

db = 10 G

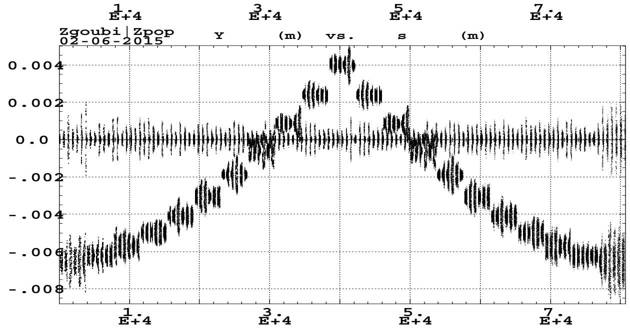

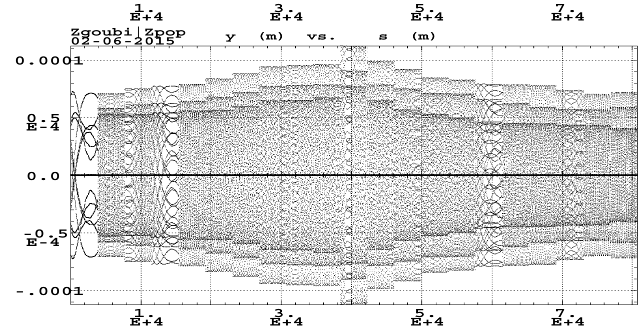

- **Beam evolution from 7.9 to 21.1 GeV and back. Starting $\epsilon_x \approx \epsilon_y \approx 50\pi\,\mu$m, $dp/p \in \pm 2 \times 10^{-4}$**

- **db =1 Gauss : Equivalent displacement is $\Delta x = \Delta B/G = 2\,\mu$m - given G=50 T/m.**

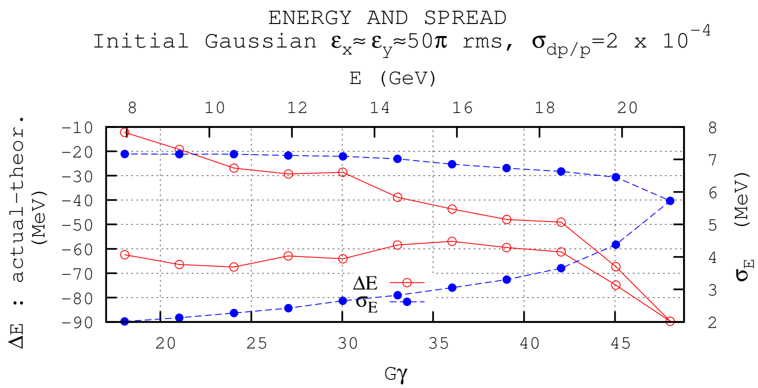

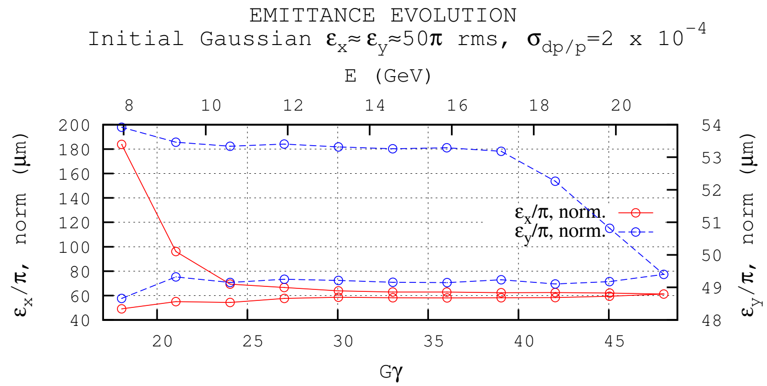

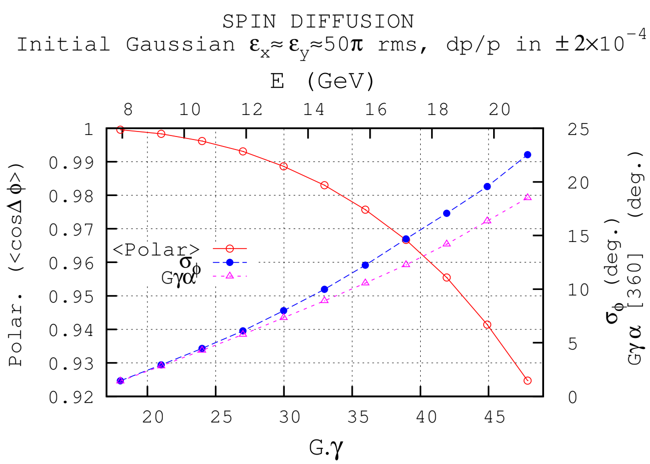

6.2 Vertical misalignment

- **Beam evolution from 7.9 to 21.1 GeV and back. Starting $\epsilon_x \approx \epsilon_y \approx 50\pi\mu$m and $dp/p \in \pm 2\times 10^{-4}$ uniform**

- **From top to bottom : dipole defect $a_0 \in [-0.1, +0.1], [-1, +1]$ G :**

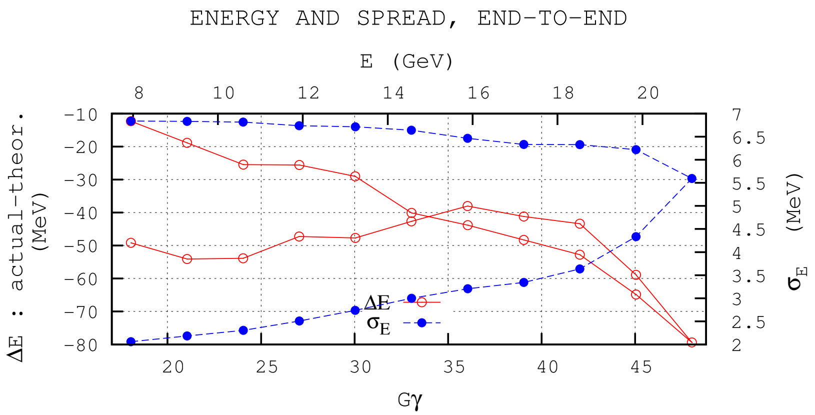

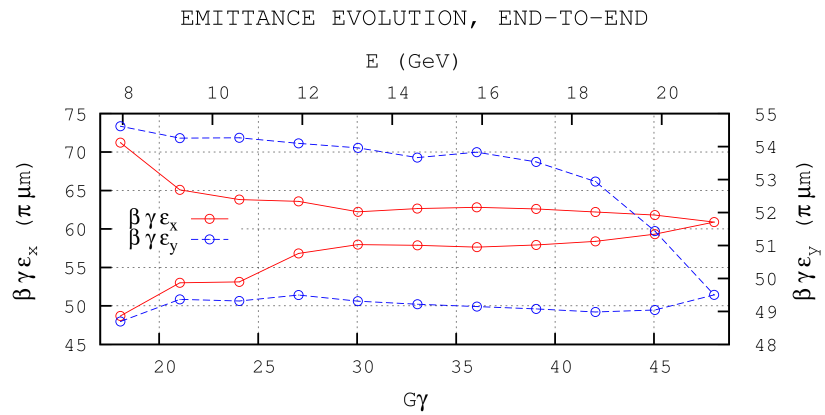

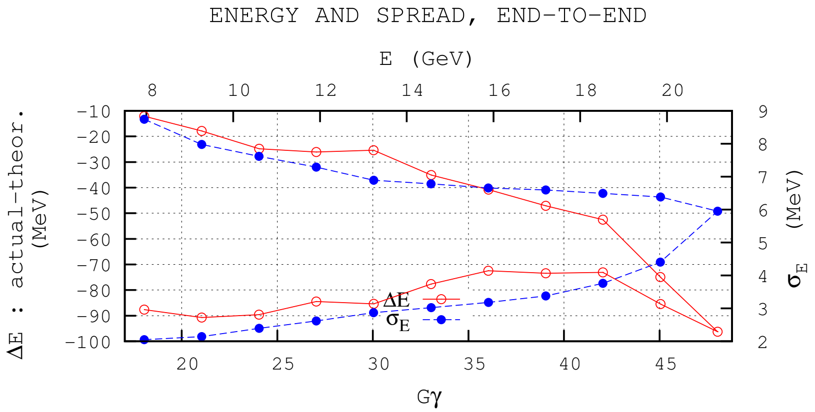

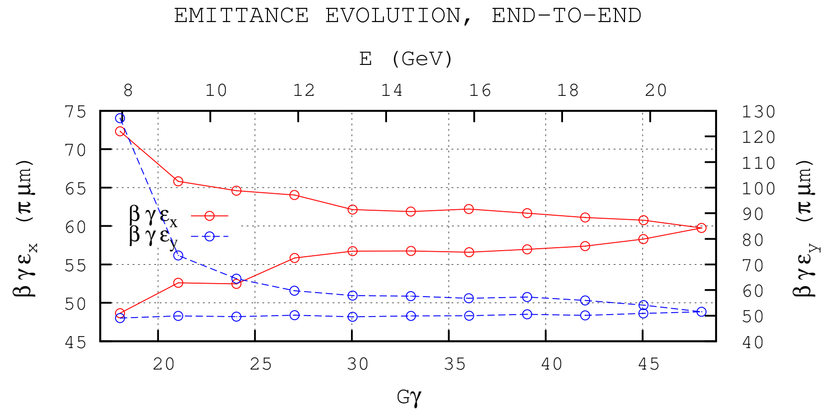

6.3 Investigating alignment error correction of a 11-beam set

• Sets of H and/or V dipole errors are generated, in cell quadrupoles, in the 6 arcs

• Error sets are taken from uniform Δb_0 and/or Δa_0 density, over

± 20 **Gauss** (± 40 μ**m equivalent misalignment)**

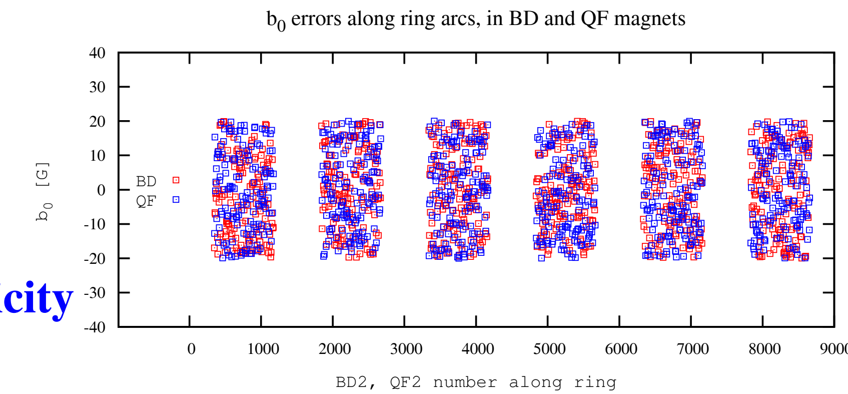

• No errors introduced in LSS neither DS - for simplicity

• These errors are corrected using brute force FIT procedure, that tweaks b_0 and/or a_0, in all QF and BD until constraints are fulfilled, namely :

- position and angle of 11 different energies
- every 23 cells in the arcs (an arc contains 138 cells, so, there are 6 such sections per arc).

• That allows 23 variables for 22 constraints (x and x' for each one of the 11 energies, in one go).

• Each 23-cell section, in all 6 arcs, is corrected in that manner. This is repeated 36 times to cover the ring.

• SR is on. Each energy is represented bu a 50 particle bunch (hence, 11×50 = 550 particles tracked in one go).

• Typical convergence of the FIT, toward the 11 theoretical orbits, for one of 36 arc sections :

```
STATUS OF VARIABLES  (Iteration #     0 /    120 max.)                ! THE VARIABLES ARE THE QF2's b_0
 LMNT  VAR  PARAM  MINIMUM      INITIAL          FINAL           MAXIMUM      STEP     NAME       LBL1     LBL2
   12    1      4  -1.000E-02   4.518E-05   4.5175080247E-05  1.000E-02  8.230E-07 MULTIPOL   QF2        MULT
   18    2      4  -1.000E-02  -5.017E-05  -5.0172080247E-05  1.000E-02  8.230E-07 MULTIPOL   QF2        MULT
   24    3      4  -1.000E-02   1.340E-04   1.3397781481E-04  1.000E-02  8.230E-07 MULTIPOL   QF2        MULT
   30    4      4  -1.000E-02  -1.333E-04  -1.3327810247E-04  1.000E-02  8.230E-07 MULTIPOL   QF2        MULT
   36    5      4  -1.000E-02   4.745E-05   4.7446188889E-05  1.000E-02  8.230E-07 MULTIPOL   QF2        MULT
   42    6      4  -1.000E-02  -1.474E-05  -1.4741066667E-05  1.000E-02  8.230E-07 MULTIPOL   QF2        MULT
   48    7      4  -1.000E-02  -2.099E-04  -2.0985586296E-04  1.000E-02  8.230E-07 MULTIPOL   QF2        MULT
   54    8      4  -1.000E-02   7.811E-05   7.8105985185E-05  1.000E-02  8.230E-07 MULTIPOL   QF2        MULT
   60    9      4  -1.000E-02  -2.761E-04  -2.7612202222E-04  1.000E-02  8.230E-07 MULTIPOL   QF2        MULT
   66   10      4  -1.000E-02   6.330E-05   6.3297133333E-05  1.000E-02  8.230E-07 MULTIPOL   QF2        MULT
   72   11      4  -1.000E-02  -1.786E-04  -1.7864781852E-04  1.000E-02  8.230E-07 MULTIPOL   QF2        MULT
   78   12      4  -1.000E-02   1.816E-05   1.8164953086E-05  1.000E-02  8.230E-07 MULTIPOL   QF2        MULT
   84   13      4  -1.000E-02   1.527E-05   1.5267744444E-05  1.000E-02  8.230E-07 MULTIPOL   QF2        MULT
   90   14      4  -1.000E-02  -5.354E-05  -5.3537733333E-05  1.000E-02  8.230E-07 MULTIPOL   QF2        MULT
   96   15      4  -1.000E-02   2.148E-04   2.1484726914E-04  1.000E-02  8.230E-07 MULTIPOL   QF2        MULT
  102   16      4  -1.000E-02  -7.791E-05  -7.7908722222E-05  1.000E-02  8.230E-07 MULTIPOL   QF2        MULT
  108   17      4  -1.000E-02   2.431E-04   2.4311473333E-04  1.000E-02  8.230E-07 MULTIPOL   QF2        MULT
  114   18      4  -1.000E-02   7.990E-05   7.9898833333E-05  1.000E-02  8.230E-07 MULTIPOL   QF2        MULT
  120   19      4  -1.000E-02   8.440E-05   8.4401917284E-05  1.000E-02  8.230E-07 MULTIPOL   QF2        MULT
  126   20      4  -1.000E-02   1.636E-04   1.6362697037E-04  1.000E-02  8.230E-07 MULTIPOL   QF2        MULT
  132   21      4  -1.000E-02   4.122E-05   4.1218400000E-05  1.000E-02  8.230E-07 MULTIPOL   QF2        MULT
  138   22      4  -1.000E-02   5.180E-05   5.1796065432E-05  1.000E-02  8.230E-07 MULTIPOL   QF2        MULT
  144   23      4  -1.000E-02   4.227E-05   4.2273506173E-05  1.000E-02  8.230E-07 MULTIPOL   QF2        MULT
 STATUS OF CONSTRAINTS (Target penalty =   1.0000E-08)
 TYPE  I   J  LMNT#       DESIRED           WEIGHT          REACHED         KI2       NAME       LBL1     LBL2         *  Parameter(s)
   3  -1 2 147    -5.7866111E-01     2.0000E-01   -5.7928530E-01   9.9814E-02 MARKER #ECellSec  *  *   2 :   1.0E+00/  5.0E+01/   Theor. x_orbit for 7.9GeV
   3  -1 3 147     5.2102765E+00     1.0000E+00    5.2105759E+00   9.1857E-04 MARKER #ECellSec  *  *   2 :   1.0E+00/  5.0E+01/   Theor. x'_orbit for 7.9GeV
   3  -1 2 147    -5.6123649E-01     2.0000E-01   -5.6144094E-01   1.0709E-02 MARKER #ECellSec  *  *   2 :   5.1E+01/  1.0E+02/   Theor. x_orbit for 9.2GeV
   3  -1 3 147     4.3105917E+00     1.0000E+00    4.3116745E+00   1.2014E-02 MARKER #ECellSec  *  *   2 :   5.1E+01/  1.0E+02/   Theor. x'_orbit for 9.2GeV
   3  -1 2 147    -5.2088326E-01     2.0000E-01   -5.1981394E-01   2.9294E-01 MARKER #ECellSec  *  *   2 :   1.0E+02/  1.5E+02/           ETC.
   3  -1 3 147     3.4780794E+00     1.0000E+00    3.4804963E+00   5.9862E-02 MARKER #ECellSec  *  *   2 :   1.0E+02/  1.5E+02/
   3  -1 2 147    -4.6023083E-01     2.0000E-01   -4.6066645E-01   4.8617E-02 MARKER #ECellSec  *  *   2 :   1.5E+02/  2.0E+02/
   3  -1 3 147     2.7061058E+00     1.0000E+00    2.7037711E+00   5.5856E-02 MARKER #ECellSec  *  *   2 :   1.5E+02/  2.0E+02/
   3  -1 2 147    -3.8142236E-01     2.0000E-01   -3.8151658E-01   2.2743E-03 MARKER #ECellSec  *  *   2 :   2.0E+02/  2.5E+02/
   3  -1 3 147     1.9880861E+00     1.0000E+00    1.9901914E+00   4.5421E-02 MARKER #ECellSec  *  *   2 :   2.0E+02/  2.5E+02/
   3  -1 2 147    -2.8634189E-01     2.0000E-01   -2.8663176E-01   2.1526E-02 MARKER #ECellSec  *  *   2 :   2.5E+02/  3.0E+02/
   3  -1 3 147     1.3189515E+00     1.0000E+00    1.3184897E+00   2.1852E-03 MARKER #ECellSec  *  *   2 :   2.5E+02/  3.0E+02/
   3  -1 2 147    -1.7668768E-01     2.0000E-01   -1.7635203E-01   2.8863E-02 MARKER #ECellSec  *  *   2 :   3.0E+02/  3.5E+02/
   3  -1 3 147     6.9385348E-01     1.0000E+00    6.9173531E-01   4.5978E-02 MARKER #ECellSec  *  *   2 :   3.0E+02/  3.5E+02/
   3  -1 2 147    -5.3767999E-02     2.0000E-01   -5.3818008E-02   6.4071E-04 MARKER #ECellSec  *  *   2 :   3.5E+02/  4.0E+02/
   3  -1 3 147     1.0858879E-01     1.0000E+00    1.1067439E-01   4.4575E-02 MARKER #ECellSec  *  *   2 :   3.5E+02/  4.0E+02/
   3  -1 2 147     8.1093355E-02     2.0000E-01    8.0888057E-02   1.0798E-02 MARKER #ECellSec  *  *   2 :   4.0E+02/  4.5E+02/
   3  -1 3 147    -4.4050766E-01     1.0000E+00   -4.3872210E-01   3.2672E-02 MARKER #ECellSec  *  *   2 :   4.0E+02/  4.5E+02/
   3  -1 2 147     2.2697555E-01     2.0000E-01    2.2728052E-01   2.3828E-02 MARKER #ECellSec  *  *   2 :   4.5E+02/  5.0E+02/
   3  -1 3 147    -9.5714321E-01     1.0000E+00   -9.5775222E-01   3.8007E-03 MARKER #ECellSec  *  *   2 :   4.5E+02/  5.0E+02/
   3  -1 2 147     3.8260641E-01     2.0000E-01    3.8335722E-01   1.4442E-01 MARKER #ECellSec  *  *   2 :   5.0E+02/  5.5E+02/
   3  -1 3 147    -1.4428212E+00     1.0000E+00   -1.4417261E+00   1.2288E-02 MARKER #ECellSec  *  *   2 :   5.0E+02/  5.5E+02/
 Fit reached penalty value   9.7583E-05
```

Matching 6 sections per arc, 6 arcs,
to 11 theoretical orbits in 1 go. Penalties.

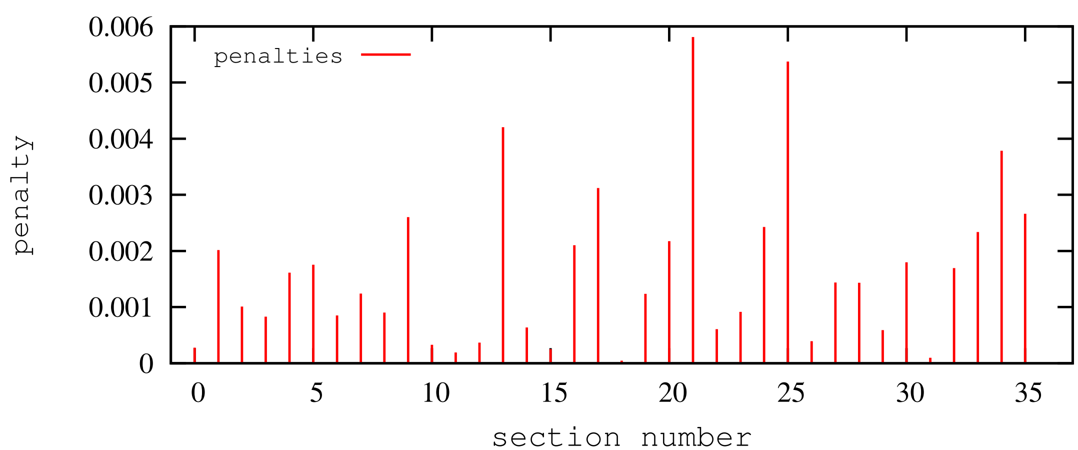

- **Sample results**

Horizontal misalignment ($b_0 \in \pm 20$ G, uniform)

Initial $dp/p = 0$, initial ϵ_x, ϵ_y zero.	**Initial $dp/p \in \pm 2\,10^{-4}$, initial ϵ_x, ϵ_y zero.**

BEFORE CORRECTION

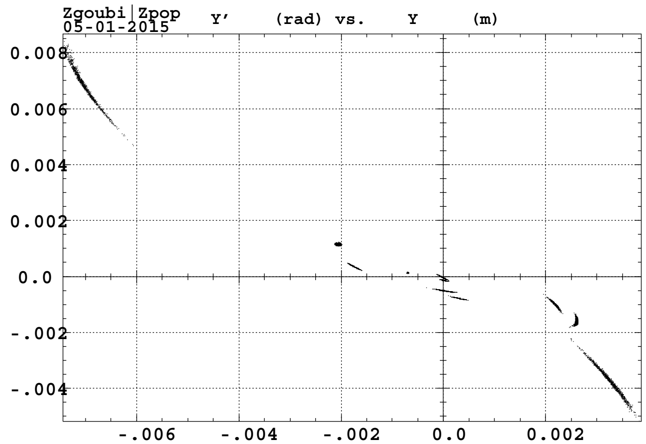

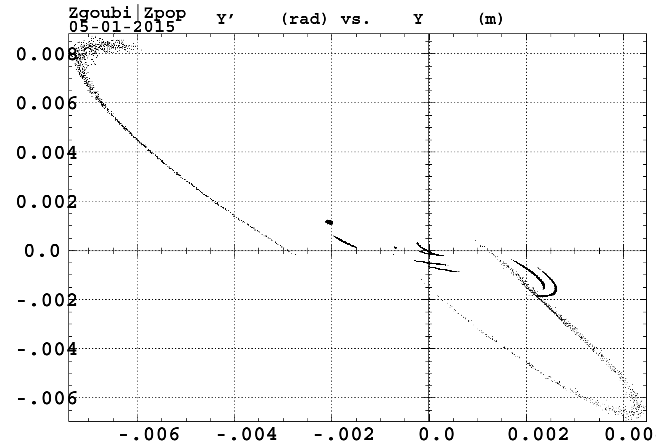

AFTER CORRECTION (Note the scales : big effect)

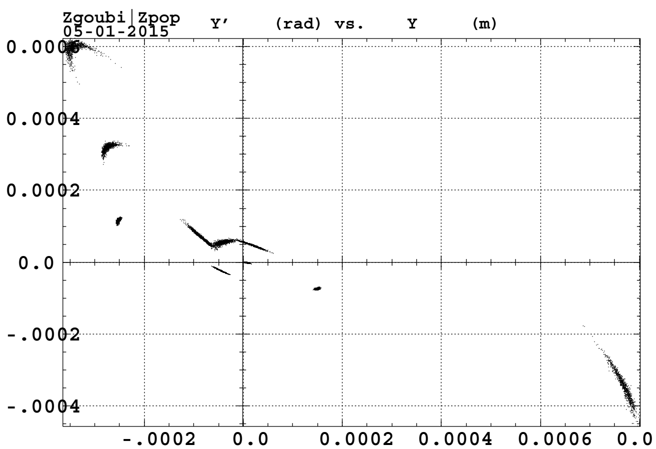

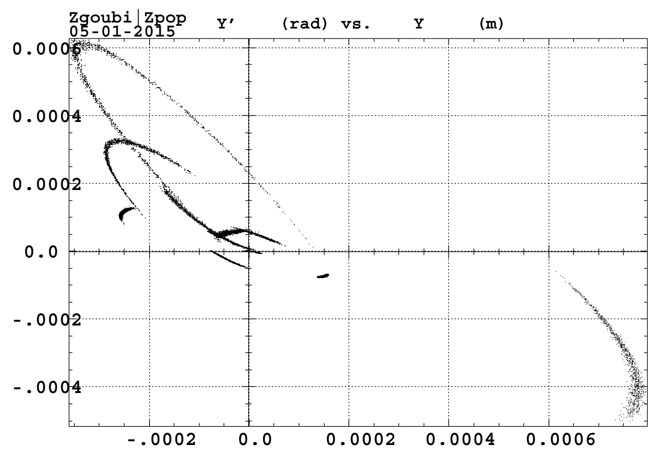

Initial $dp/p = 0$, initial ϵ_x, ϵ_y 50pi.

Initial $dp/p \in \pm 2\,10^{-4}$, initial ϵ_x, ϵ_y 50pi.

BEFORE CORRECTION

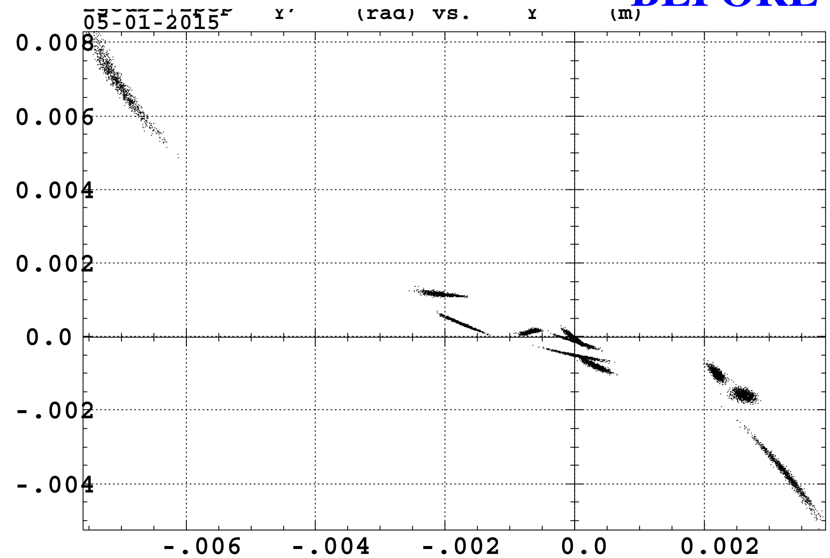

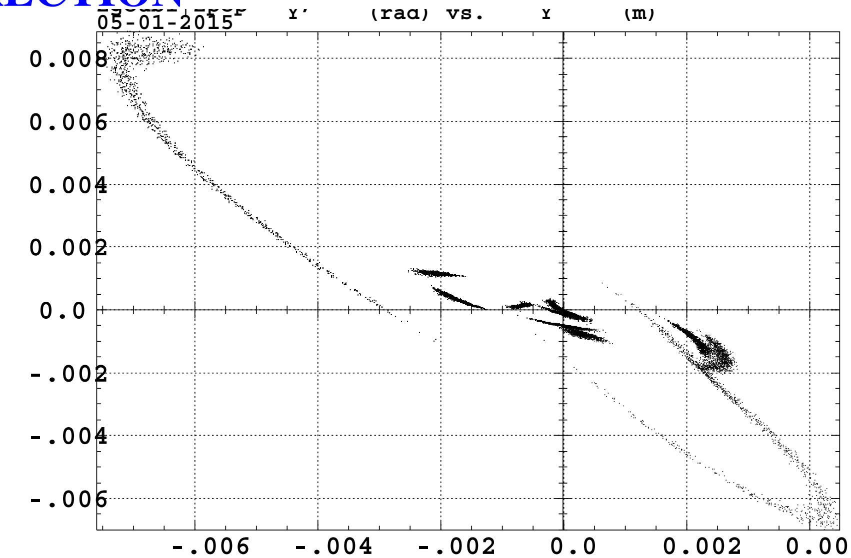

AFTER CORRECTION (Note the scales : big effect)